POLITECNICO
MILANO 1863

SCUOLA DI INGEGNERIA INDUSTRIALE
E DELL'INFORMAZIONE

CO_2-Based Mixtures as Working Fluids for High-Temperature Heat Pumps and Thermally Integrated PTES Applications

Tesi di Laurea Magistrale in Energy Engineering – Power Generation

Renzoni, Mario, 10869093

Advisor:
Prof. Dario Alfani

Co-advisors:
Ettore Morosini

Academic year:
2023-24

In response to the urgent need for sustainable energy solutions, High-Temperature Heat Pumps and Pumped Thermally Energy Storage systems are promising technologies for industrial heating processes and large-scale energy storage, respectively. This thesis explores the potential of CO_2-based mixtures in HTHPs, aiming on optimize performance and efficiency for industrial applications. A significant innovation lies in proposing a novel technological solution for heat pumps, utilizing an expander to improve COP and recover part of the work expended by the compressor. The performance of these system was analyzed across a large spectrum of operating parameters and plant assumptions. Results, presented through heatmaps for different configurations, demonstrate how the utilization of the expander enables significantly higher COPs with improved second law efficiencies. This leads to an advantage not only for high-temperature heat delivery processes but also for thermally integrated PTES systems, providing significant benefits to RTE. The research also involves calibrating and validating a numerical model using the Peng-Robinson Equation of State to define thermodynamic properties of mixtures, aiming to be a useful tool for their definition. Different case studies are investigated to propose efficient applications, both for HTHP and PTES. The entire study, including numerical simulations and model development, is conducted using MATLAB.

Keywords: High Temperature Heat Pump, CO_2-based Mixtures, Peng-Robinson, Pumped Thermal Energy Storage

1. Introduction

In recent years, global energy consumption has strongly increased, with a fast rise of greenhouse gases emissions [1]. The progressive increase of climate-related risks has driven countries to develop energy policies and sustainable strategies towards their reduction [2], and renewable energy has emerged today as the best prospect for ensuring clean energy, mitigating carbon emissions [3]. The ongoing integration of renewables, known for their significant unpredictability and variability, brings about additional costs related to the start-up of thermal units when necessary and the rapid power output increase that may be requested to cover supply and demand unbalance [4]. Energy demand management runs so parallel to the persistent search for innovative technological solutions to drive the decarbonization process [5]. Aligning with ambitious targets and commitments towards carbon neutrality, *High Temperature Heat Pumps* (HTHP) prove significant potential for utilization of off-peak electricity and low-grade waste thermal energy, offering a fresh perspective on the decarbonization of industrial heating, leading to a reduction of CO_2 emissions up to 30-40% if linked to the exploitation of renewable heat sources and industrial low-temperature waste heat [6]. Furthermore, to effectively handle significant quantities of variable electricity generated from renewable sources and guarantee the security of energy supply, large *Energy Storage Systems* (ESS) combined with thermal cycles, also represents an option to store electricity [7], releasing it when demand is greater than supply. According to the form of energy stored, different solutions for ESS have been developed. Carnot Batteries, also known as *Pumped Thermal Energy Storage* (PTES), boasts different advantages, such as the absence of geographical restrictions, high energy density and lower size of fluid vessels [8]. PTES systems consist of a heat pump which uses electricity to move heat from a low-temperature source to a high-temperature one during charging, then converts stored heat back into electricity during discharge, enabling efficient thermal energy conversion.

Particularly, CO_2 HTHP have attracted increasing interest in the last couple of years for many applications moving the attention on possible innovative solutions involving the use of CO_2 HP to cover the thermal input required by specific industrial applications or to store heat to be delivered by a thermal cycle. The utilization of carbon dioxide as a working fluid brings both challenges and opportunities, with its properties making it particularly interesting if integrated into thermodynamic cycles designed for power generation or cooling applications. On one hand, carbon dioxide is a natural refrigerant, non-toxic, with a low *Global Warming Potential* (GWP) and zero *Ozone Depletion Potential* (ODP), fully available in atmosphere, but its low critical temperature makes difficult to adopt subcritical configurations [9]. Some studies show how is possible to optimize the performance of a heat pump, finding a maximum for the *Coefficient of Performance* (COP) for a certain optimum discharge pressure [10] and applications combined with supercritical CO_2 for ranges of higher temperature and with trans-critical CO_2 for lower temperatures are today widely investigated [11].

This thesis aims so to analyze the thermodynamic potential given by using CO_2-based mixtures for HTHP applications and CO_2 PTES systems, trying to overcome limitations of pure carbon dioxide by adding small amounts of dopants with higher critical temperatures, modifying the thermodynamic properties of the pure fluid [12]. The use of mixtures exhibits a variable phase change temperature, which enables them to closely match the temperature profile of the working fluid with both the sensible heat sink and heat source. Consequently, this minimizes exergy destruction and enhances the performance of the heat pump [13]. CO_2 mixtures are being studied to understand the parameters that optimize COP, including composition, compression ratio, and temperature glide. The search for an optimal working fluid and design parameters is thus not carried

out only for high-temperature applications in industrial processes but also for PTES systems, with a more refined focus on finding the best coupling between the charge and discharge fluids.

The major innovation of the work lies in both proposing an innovative technological solution for the heat pump, exploiting an expansion that ensures an advantage in COP and partially recovers the work spent on compression, and in the calibration and validation of a numerical model using the *Peng Robinson Equation of State* (PR EoS) to define the thermodynamic properties of a generic mixture. Most of calculations proposed are developed with REFPROP distributed through the NIST Standard Reference Data program [14]. Despite its wide usage, it has some limitations, including potential gaps in fluid coverage and accuracy outside validated conditions, as well as considerations regarding cost and computational resources. What suggested the development of a proper numerical model for calculating the thermodynamic properties of mixtures is indeed the ability to adapt it to every class of fluid, presenting itself as an accessible model with a strong possibility of customization, according to the user's needs, with the potential for further developments. The versatility of the model lies in its ability to adapt fluids of any type, the experimental data of which can be derived from existing literature. These data are then used to calibrate the model, ensuring better results. The model's potentialities are different, extending beyond the definition of individual thermodynamic points to solving complete thermodynamic cycles through numerical models whose validation will be accurately described. As mentioned, the possibility of making the heat pump system more complex in both recuperative and non-recuperative configurations will be analyzed, determining the actual advantage achievable on COP different configurations. Additionally, various case studies with different fluids will be investigated, seeking, and proposing potentially efficient applications. Finally, a case study will be associated with the search for a feasible configuration for the PTES, using a CO_2 mixture as charge fluid coupled with a pure discharge one, exploring the conditions to ensure its best *Round-Trip Efficiency* (RTE). The entire study and all the numerical codes have been completely developed using MATLAB, and experimental data for model calibration was obtained from literature.

2. High Temperature Heat Pumps (HTHPs)

Within industrial contexts, energy savings involve *waste heat recovery* (WHR), with a strong focus attributed to the advancement of an efficient technology which permits its exploitation, as *Organic Rankine Cycle* (ORC) where thermal recovery process typically targets temperatures ranging approximately from 100°C to 400°C [15]. ORC applications, using waste heat sources at temperature lower than 85 °C are rare, with efficiencies and profitability widely investigated in [16, 17], making them not suitable for conversion into electric power. An interesting perspective is to upgrade or recycle these low-grade waste heat sources raising their temperature up covering heat demand of many industrial processes.

HP technologies, which have been proposed and investigated for this purpose [18], can be categorized according to the temperature threshold of the heat they generate. Drying processes, distillation, and steam production are examples of possible industrial applications for which heat pumps can be adopted to deliver heat [19]: theoretical application potential for the use of heat pumps in industrial processes may be estimated by evaluating the heat demand of each industrial sector and the temperature levels of the applied processes [18], and an interesting and comprehensive analysis of the possible configurations such as multi-stage compression or solution with ejectors replacing the expansion across the valve is reported in [20]. Once the heat output overcome 100 °C, literature typically refers to HTHPs [21], which emerge as a perspective technology with a great potential in supplying clean heat to energy intensive industrial processes, upgrading low-grade

waste heat at temperatures up to 200 °C [22]. Current trends for HTHPs are centered on the development of new refrigerants characterized by low GWP and low ODP at temperatures ranging from 150 to 250°C, with HTHP technologies capable of providing a heat sink temperature of 160°C are already commercially available [23]. The primary threshold lies in developing compressors capable of operating at higher temperatures [24], with the outlet temperature generally limited to 180 °C to avoid thermal decomposition of its lubricant [25]. Another challenge is selecting a refrigerant with high performance, low GWP and zero ODP. While hydrofluoroolefins (HFOs) are proposed, they pose environmental risks at higher temperatures [26]. Natural refrigerants like water, ammonia, CO_2, and hydrocarbons have limitations such as high pressures, flammability, or cost. Finding an ideal refrigerant meeting thermal, environmental, safety, efficiency, and availability criteria remains a significant challenge for HTHP development [27]. For our intents, there are currently several research works on mixtures as working fluids for HTHP systems [28], while purpose of this work is to investigate on CO_2-based mixture HTHP application and the possibility to extend the range of temperature at which mixtures may deliver heat up to 200 °C with higher performance avoiding risks for fractionation.

2.1 Heat pump cycle configuration and design considerations

Common configurations of heat pumps often present a single compression stage. In this setup, vapor coming from the evaporator undergoes compression to achieve higher pressure, transfers heat to the condenser prior to being expanded in lamination valve, a process that may be regarded as an isenthalpic expansion. Other possible solutions involve incorporating a recuperator, as depicted in Figure 2.1. After evaporation the working fluid is superheated in the recuperator by recovering the residual heat from the stream at the condenser outlet, then compressed and cooled. After the additional cooling in the high-pressure side of the recuperator, the working fluid completes the thermodynamic cycle by an expansion through the valve, before entering again into the evaporator to absorb heat from a low-grade waste heat source.

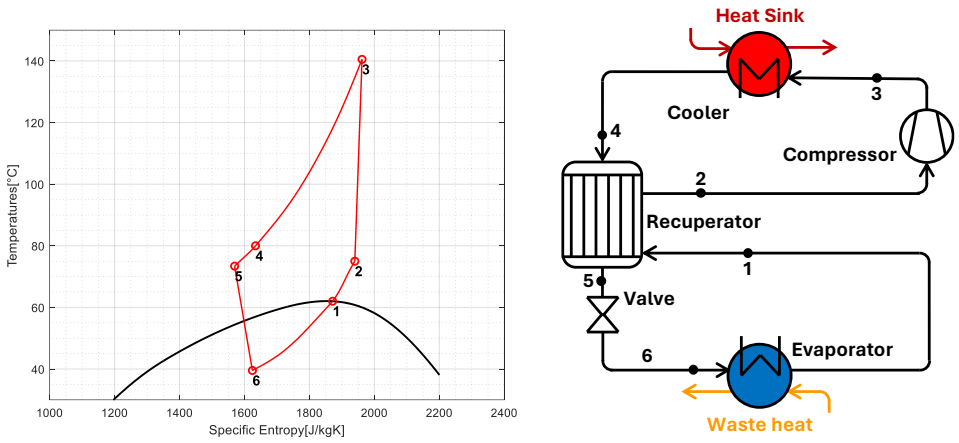

Figure 2.1 Recuperative High Temperature Heat Pump layout and its corresponding Ts diagram.

Enhanced energy efficiency is obtained with a recuperative HTHP, reduced operational costs, lower carbon emissions, increased energy resource flexibility [29], allowing for higher COP in defined conditions as studied in the next sections. Both the evaporator and condenser pressures define the thermodynamic behavior of the system. When working with mixtures, the composition also becomes an important variable to optimize, as the amount of dopant present alters the fluid properties and consequently, the average working pressures and temperatures. Furthermore, the advantage of working with mixtures is related to their non-variable phase change, allowing a better match with the temperature profile of both the sensible heat sinks and sources, thereby reducing

exergy destruction, and enhancing heat pump performance [30]. Therefore, the temperature glide at the evaporator and condenser must also be controlled to meet the heating constraints provided by the sink or source. If the system is recuperative, also the pinch point or the effectiveness of the recuperator are parameters that impact the system's efficiency, and their design value generally depends on techno-economic considerations. This set of variables is the primary to be optimized with the aim of defining a HP performance map across its proposed configurations. Another efficiency advantage can be achieved by considering the possibility of incorporating an expander to reduce efficiently the pressure after condensation.

Specifically, the proposed solution involves an initial expansion stage that brings the mixture in conditions of saturated liquid. This aims to recover useful work that can be supplied back to the compressor and conclude the expansion through valve throttling. The configuration, whether in recuperative or non-recuperative asset, should inherently provide a higher heating-COP and lower irreversibility, reducing the Δp to be accomplished through the valve. However, such solutions aren't typically adopted due to limited recoverable energy and challenges associated with designing and operating two-phase flow expanders. The use of radial piston machines used as expanders has been investigated, showing promising results with efficiencies ranging from 80-85% under normal conditions [31]. Additionally, several other devices have been developed, including scroll-type expanders [32], or turbo expanders [33].

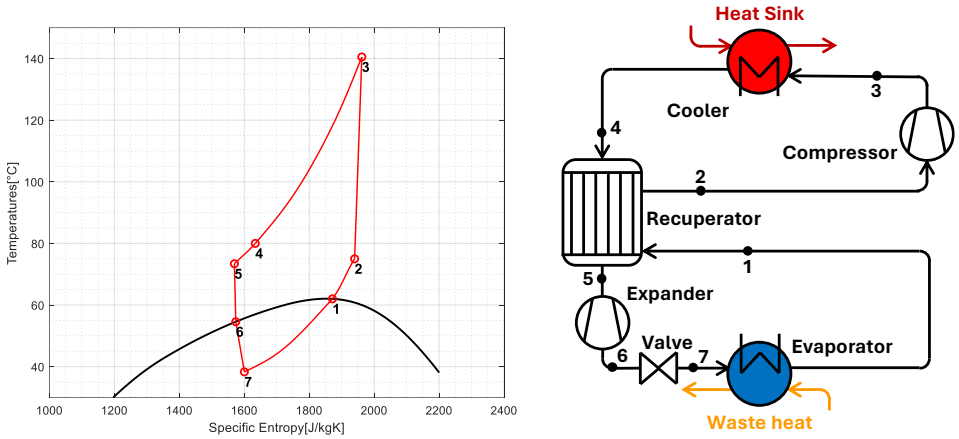

Figure 2.2 Recuperative High Temperature Heat Pump layout with expander and its corresponding Ts diagram.

3. Numerical modelling of the Heat Pump cycle

In this section are discussed the main optimization algorithms and calculation procedures employed for various heat pump configurations. HTHP is numerically modelled by defining the following thermodynamic conditions and components' parameters:

- **Inlet state of the heat source**, which defines the outlet evaporator temperature. It depends on the temperature at which the waste heat source is available. A minimum pinch point of typically 5°C is assumed.
- **Inlet state of the heat sink**, which defines the temperature at the end of the trans-critical cooling of the working fluid. A minimum pinch point of typically 5°C is assumed.
- **Maximum pressure of the HP p_{max}**, which defines, given the compressor inlet condition imposed, the compression ratio of the heat pump.
- **Pressure losses Δp**, in the main heat exchangers (and recuperator). If the configuration is recuperative, also ΔT_{pp}, fixed at the hot end of the recuperator, and the pressure losses both at cold and hot side of the component are fixed.

- **Isentropic efficiency** $\eta_{is,exp|comp}$, considered fixed and fluid independent [34], for the compressor (and expander).

The variables that characterize the thermodynamic behaviour of the system are listed and their variations are commented through next sections to understand how the COP is affected:

1. Minimum pressure of the HP p_{min}, at which the evaporation occurs.
2. Compression ratio β_{comp} of the compressor.
3. Expansion ratio β_{exp} of the expander.
4. Sink and source glide $\Delta T_{sink}, \Delta T_{source}$
5. Composition of the binary CO_2-based mixture used as working fluid.

All fluids and mixture properties can be obtained through REFPROP V10 or through the PR EoS model developed within this thesis work.

3.1 Simple Heat Pump layout

After initial assessment of the thermodynamic input variables, it is verified that the compressor's inlet conditions correspond to saturated vapor. In that sense, an iterative process is necessary to adjust the outlet evaporator temperature.

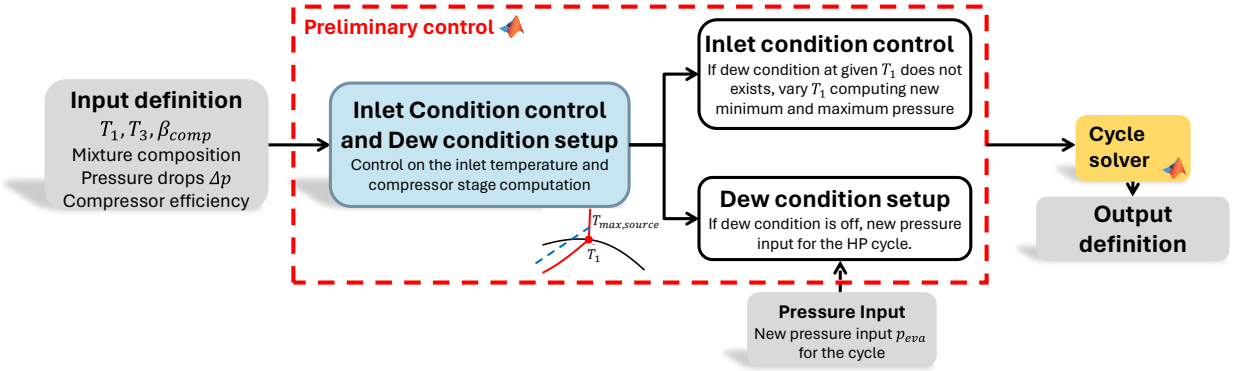

Figure 3.1 Numerical solving approach for HTHP. Inlet condition control.

As shown in Figure 3.1, T_1 is defined as the difference between $T_{max,source}$ and $\Delta T_{pp,source}$, not subject to optimization but fixed and adjusted through the algorithm control. This is because, for a given mixture composition, it might not be possible to define a condition of saturated vapor at the assigned temperature. Consequently, T_1, is set equal to the cricondentherm for the mixture at composition assigned. In the Figure 3.2 is depicted the methodology developed to solve numerically the heat pump cycle.

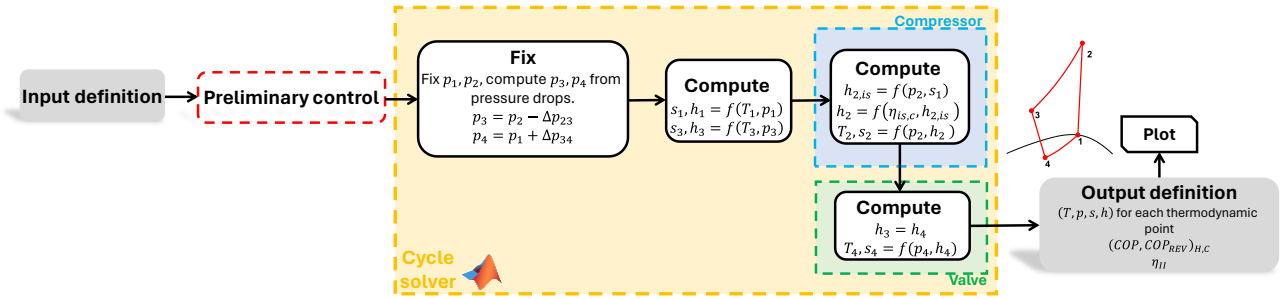

Figure 3.2 Numerical solving approach for HTHP. Simple Layout numerical solver.

The decision regarding recuperative or non-recuperative arrangement, or the implementation of an expander-based solution, can be specified as input parameters. The optimization logic for such

choices will be detailed in the next sections. Valve throttling is characterized by ensuring equal enthalpy at the inlet and outlet, with knowledge of the upstream and downstream pressures. Also, the resolution of compression is established through the determination of its isentropic efficiency.

3.1.1 Thermodynamic analysis

COP is generally considered a common performance indicator for heat pump systems: the higher is the COP, the lower the electricity consumption (and thus the electricity cost) for running the compressor for the same heat duty. Maximum COP achievable depends on the range of temperature in which the heat pump works, therefore the second law efficiency relates the COP to the maximum achievable [35]. Specifically, the heating-COP is defined as the ratio between the energy exchanged with the hot sink $\dot{Q}_{sink}$ and the energy introduced by compressor $\dot{W}_{compressor}$ as defined in Equation 1.

$$COP_{heating} = \frac{\dot{Q}_{sink}}{\dot{W}_{compressor}} \tag{1}$$

For evaluating the reversible-COP, Lorenz cycle is chosen as reference, as Carnot one is not a reliable reference in case of variable temperature heat sinks, as in this case, considering the irreversibilities associated to heat transfer. As literature reports, Lorenz identifies a cycle operating as the Carnot one with an isentropic compression and expansion between and with heat transfer process that occurs at a thermodynamic average temperature T_{mln} that might be approximated by the logarithmic mean temperature for both hot and cold stream [36].

$$COP_{rev,heating} = \frac{T_{mln}(T_{hot-end};T_{cold-end})_{hot}}{T_{mln}(T_{hot-end};T_{cold-end})_{hot} - T_{mln}(T_{hot-end};T_{cold-end})_{cold}} \tag{2}$$

Lorenz efficiency then gives an indication about how close the performance of the heat pump is compared to the maximum achievable performance. Considering the Equation 2, the second law efficiency is reported below.

$$\eta_{II} = \frac{COP_{heating}}{COP_{rev,heating}} \tag{3}$$

3.2 HTHP with expander solution and optimization algorithm

The innovation and proposal involve the integration of an expander, with the aim of improving the COP, as expressed in Equation 4. The expander is inserted at the outlet of the condenser, or the recuperator if present. The addition of the expander allows recover a portion of the work spent in compressing the mixture. The proposed system includes:

1. Expansion from maximum pressure to saturated liquid conditions is implemented to avoid potential issues associated with the expansion of a two-phase mixture, avoiding risks such as erosion which can degrade the performance of the expander and even damage the system.
2. Valve throttling down to minimum pressure conditions, accounting for pressure drop losses within the evaporator.

For that particular configuration the COP is considered as:

$$COP_{heating} = \frac{\dot{Q}_{sink}}{\dot{W}_{compressor} - \dot{W}_{expander}} \tag{4}$$

An algorithm for calculation and optimization is designed to assess expander outlet conditions through an iterative process, as illustrated in Figure 3.3. The calculation logic is closely similar to the previously described approach, with the key difference that, following the definition of thermodynamic conditions at the compressor outlet and at the end of the cooling (see Figure 2.2), the process continues through an iterative solving procedure. Once the isentropic efficiency of the expander is determined, the thermodynamic conditions at the expander outlet, under saturated liquid conditions, are derived to meet the specified tolerance on efficiency.

The process involves a guess-and-check method until the correct condition is found, ensuring that the expansion occurs with the assigned efficiency, within a certain tolerance. Internally, there are control steps to guarantee that only valid scenarios are considered, rejecting cases where the expander's inlet conditions are already in a two-phase state. Once evaluated the expander outlet condition, the loop is closed evaluating missing thermodynamic points of the cycle evaluating the main performance parameters. To reduce computational time, particularly when the cycle is solved using the PR-based model, a database is generated containing saturation curves of the mixtures under investigation for performance analysis. A fine grid is created, with a certain Δ assigned, and for the expander exit condition optimization algorithm, only thermodynamic points on the curve with entropy greater than the turbine inlet entropy are considered.

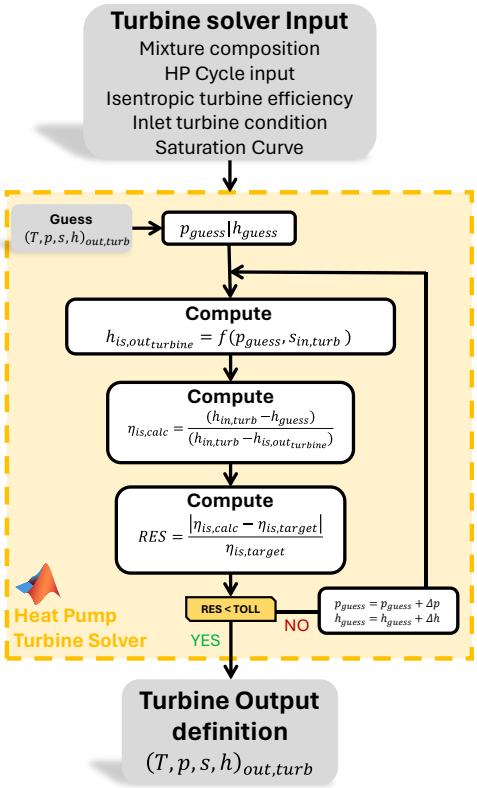

Figure 3.3 Numerical solving approach for HTHP. Expander numerical solver.

3.3 Recuperative Expander-based Heat Pump layout

Regarding the recuperative solution, the design strategy, presented in Figure 3.4, is common and is based on the choice of the pinch point temperature ΔT_{pp}, fixed at its outlet, and the pressure losses Δp_{rec} occurring in it. Furthermore, the optimization of the outlet recuperator condition is based just on thermodynamic calculations, avoiding in this first analysis detailed considerations on the component's architecture and geometric parameters, as all the components of the system. When adopting a technology that involves the use of a recuperator, the order at which thermodynamic

points are defined changes, depending primarily on optimizing the exit conditions from the recuperator on both sides. This is because the exit conditions from the compressor cannot be predetermined now, as they are closely linked to the inlet conditions, which remain unknown until the balance at the recuperator is closed.

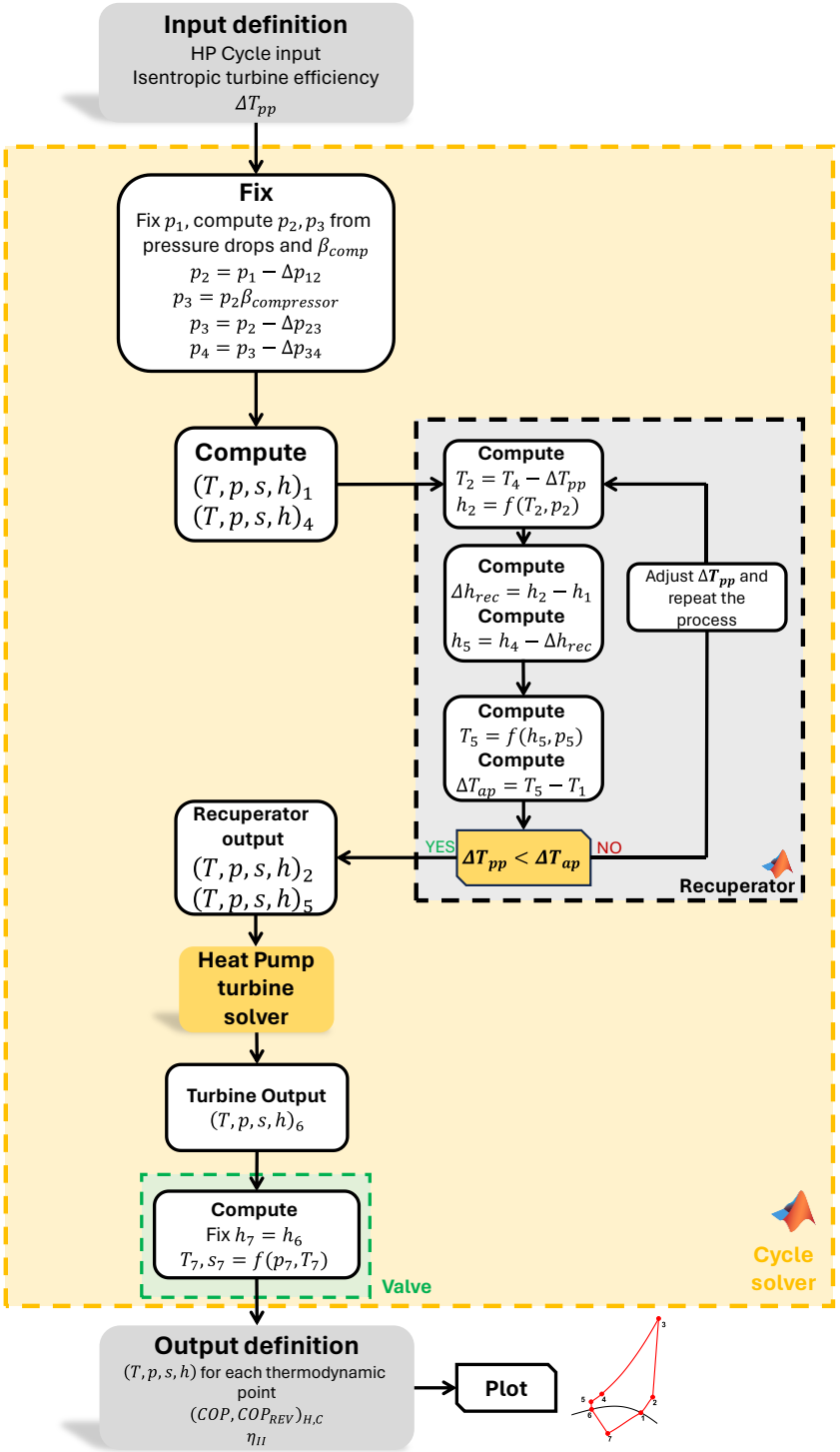

Figure 3.4 Numerical solving approach for HTHP. Expander-Recuperative numerical solver.

Furthermore, if we consider a solution that incorporates the expander, its inlet conditions need to be defined. The only fixed variables are the inlet conditions of saturated vapor into the recuperator, as they are fixed input variables, and the hot side inlet temperature of the recuperator. Adopting a recuperator, the compressor inlet temperature increases, just defined through Equation 5, ensuring

some performance advantages under certain conditions, particularly if the temperatures allow operation in a recuperative mode. Consequently, given a fixed pinch point, defined the condition at the hot side of the recuperator, holds that:

$$T_{in,comp} = T_{in,rec}^{HOT} - \Delta T_{pp} \tag{5}$$

Considering the most complex solution proposed (see Figure 3.4), T_2 is the inlet compressor temperature $T_{in,comp}$, while T_4 is the hot side inlet recuperator temperature $T_{in,rec}^{HOT}$. Once the thermodynamic conditions at the cold side exit of the recuperator are defined, the enthalpy variation is calculated, thus the enthalpic balance is closed through Equation 6 to determine all the inlet and outlet conditions of the recuperator.

$$(h_{in} - h_{out})_{rec}^{HOT} = (h_{out} - h_{in})_{rec}^{COLD} \tag{6}$$

Finally, the approach point ΔT_{ap} is determined, verifying if the assumption that the pinch point occurs at the cold hot side of the recuperator is feasible.

4. Thermodynamic computation for CO_2-based mixtures

Advanced resolution models are implemented by REFPROP, featuring an extensive database and a range of fluids, including mixtures and properties that can be defined. The interface program allows rapid calculations, being the basis of the methodology proposed in the previous section. Similarly, a model based on the PR EoS has been developed, aiming to achieve various objectives, including thermodynamic calculations for any type of fluid without constraints related to the presence of the fluid in a program database. Instead, fundamental properties necessary for solving the EoS are defined through MATLAB. To this end, a calculation model has been implemented, defining a series of algorithms, and calibrating the model using experimental data obtained from the previous state of the art for both mixtures and individual pure components. Through rigorous analysis and validation, this section tries to establish the efficacy and reliability of the proposed calculation model in thermodynamic analyses. As expressed, its implementation has been possible using MATLAB, employing a series of a series of optimization and resolution algorithms for computing all the thermodynamic essential quantities for solving a process flow diagram and conducting basic thermodynamic calculations. The Peng-Robinson formulation utilized is readily available in the common state-of-the-art literature [37] [38] and reported in the final appendix.

Specifically, the fundamental points of the model are here highlighted:

1. Establish a computational logic for defining Vapor-Liquid Equilibrium (VLE) conditions accurately, as well as determining bubble and dew point conditions.
2. Develop an algorithm to optimize the *binary interaction parameters* k_{ij} (BIP), which characterize the molecular interactions between the molecules of both species of the mixture.
3. Definition of thermodynamic quantities from volumetric one such as pressure and temperature and vice versa, through extrapolation techniques using MATLAB solvers like *fsolve* or *lsqnonlin*.
4. Implementation of PR to solve HP-based mixture systems.

It was necessary to establish a formulation for the specific heat of ideal gases. A NASA 9-coefficient polynomial parameterization is used to compute the species reference-state thermodynamic properties [39].

$$\frac{c_p^{\circ}(T)}{R} = a_0 T^{-2} + a_1 T^{-1} + a_2 + a_3 T + a_4 T^2 + a_5 T^3 + a_6 T^4 \quad (7)$$

Thermodynamic quantities were then calculated as a sum of the corresponding one calculated under ideal gas conditions and a residual term, whether it be enthalpy or entropy. These formulations, as adopted, are detailed in the appendix, and defined based on available literature [40] .

4.1 VLE computation and BIP optimization

The first step aims to define an approach for computing conditions under *Vapor-Liquid Equilibrium* (VLE). To utilize the PR model for predicting CO_2-based mixture properties accurately, it's essential to determine precise values of k_{ij} through fitting experimental data for the mixture to investigate. Hence, is important to get a significant volume of experimental data from published literature. For the intended purpose, it was decided to utilize experimental data obtained at various temperatures, which also reported dew and bubble compositions evaluated at different pressures.

For optimizing BIP, the objective is to align PR predictions as closely as possible with experimental data. Consequently, is mandatory to define an objective function F [41], formulated in Equation 8.

$$F = \frac{1}{N}\sum_{i=1}^{N}\left(\left(\frac{|P_{exp} - P_{calc}|}{P_{exp}}\right)^2 + \left(|y_{exp} - y_{calc}|\right)^2\right)^{0.5} \quad (8)$$

where N represent the quantities of experimental data fitted for VLE, and the subscripts *exp* and *calc* refer to the experimental and PR calculated values at the given composition. Moreover, to quantify the disparity between calculated values and experimental data, other statistical parameters are considered in Equation 9 and Equation 10.

The *absolute average relative deviation* (AARD) indicates the relative deviations of the bubble pressure calculated from the experimental one, and the *average absolute deviation* (AAD_y) the absolute one of vapor molar fraction.

$$AARD = \frac{1}{N}\sum_{i=1}^{N}\left(\frac{|P_{exp} - P_{calc}|}{P_{exp}}\right) \times 100\% \quad (9)$$

$$AAD_y = \frac{1}{N}\sum_{i=1}^{N}\left(|y_{exp} - y_{calc}|\right) \quad (10)$$

For the computation concerning bubble conditions and the associated optimization algorithm for calculating BIP, liquid mole fraction is assumed known at the assigned temperature, then an iterative process developed upon a *Newton's numerical resolution method*, based on PR EoS formulation is used to build the solution. As a result, the output provides the bubble pressure and the corresponding vapor-phase composition. The process for BIP optimization follows a similar approach. Initially setting a value for k_{ij}, the calculation is repeated multiple times using guessed values of y and p_{bubble} defined from experimental data. For each assigned value, the bubble pressure and y are calculated for each temperature, identifying the optimal value for k_{ij} in the one corresponding to the minimum value of F. Additionally, $AARD$ and AA_y are reported. To clarify, the dew point conditions are calculated by setting the conditions in the vapor phase and iterating over the liquid mole fraction.

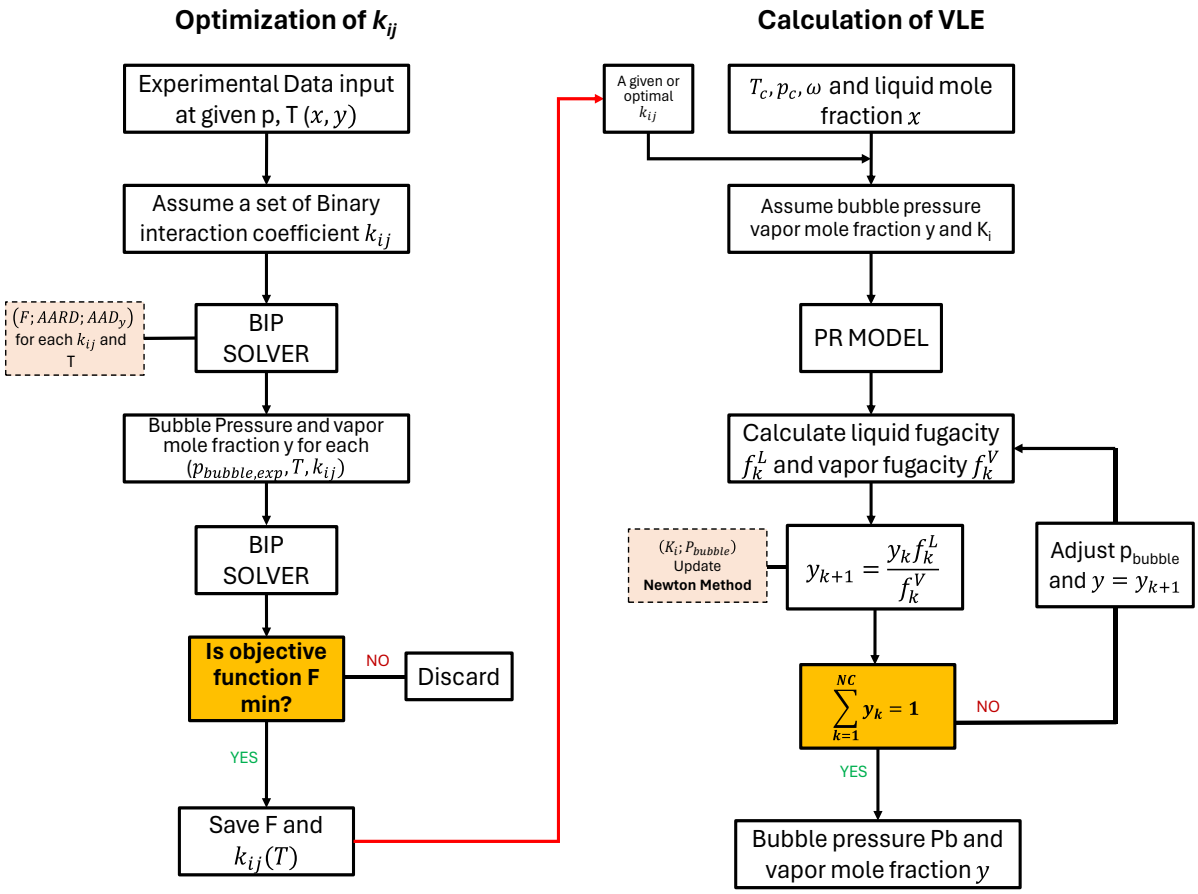

Figure 4.1 Flow diagram for bubble property calculation and optimization of kij.

The ultimate goal is to define a function that describes the behaviour of the interaction parameter as a function of temperature. To achieve this, once the optimal BIP at a given temperature is determined as described, the MATLAB *curvefitter* tool is employed, where the choice between linear (*poly1*) or quadratic (*poly2*) approximation is made based on the criterion of *maximum likelihood estimation*, a statistical approach used for estimating the parameters of a probability distribution given observed data.

To validate the optimization algorithm, reference is made to CO_2-Acetone and CO_2-Propane mixture, where experimental data and expected results comparison are obtained from [42] and [43] respectively. Comparisons between the predicted values and the experimental data are so presented in the of Table 4.1 for a CO_2-Acetone mixture. At a given temperature, the isothermal VLE curves of CO_2 mixtures only exist in a certain range of CO_2 molar fraction as and this range generally decreases with temperature as is clear from Figure 4.2 and Figure 4.4. When considering $k_{ij,opt}$, the isothermal dew and bubble pressure curves exhibit a good alignment with the experimental data.

$k_{ij} = k_{12}^{(0)} + k_{12}^{(1)} * T$	$k_{12}^{(0)}$	$k_{12}^{(1)}$
Studied Value	0.01181	-3.6 x 10^{-5}
PR model Value	0.01259	-3.2 x 10^{-5}

Table 4.1 Comparison of coefficients of the binary interaction parameter k_{12} for a CO_2-Acetone mixture, obtained in this study, and in the study proposed by Gisselle E. et al. in [42].

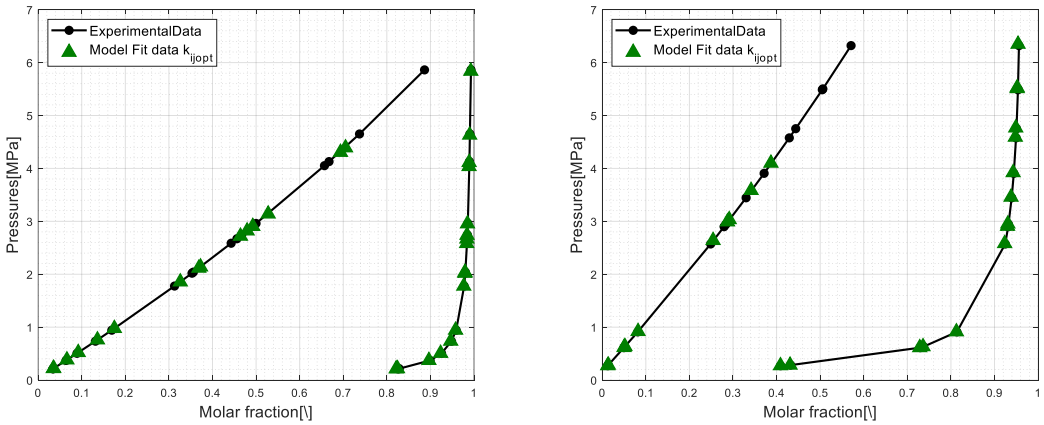

Figure 4.2 P-xy phase equilibrium diagram for a CO_2-Acetone at 303.15 K and 343.15 K: solid line, liquid, and vapor composition experimental data; (Δ) this study.

Conversely, when k_{ij} is not optimized, the bubble pressure curve significantly diverges. This can be better illustrated using a CO_2-Propane mixture, as depicted in Figure 4.4.

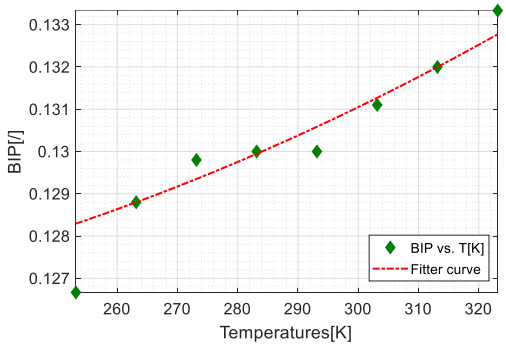

Figure 4.3 Optimum values of k_{ij} versus temperature fitted for a CO_2-Propane mixture.

Moreover, at a given temperature, k_{ij} demonstrates a greater influence on the accuracy of bubble pressure predictions. Regarding the dew pressure, as the molar fraction of CO_2 increases, the disparity between $k_{ij,opt}$ and null k_{ij} expands.

Consequently, to precisely compute mixture properties, optimizing k_{ij} through fitting experimental data is fundamental.

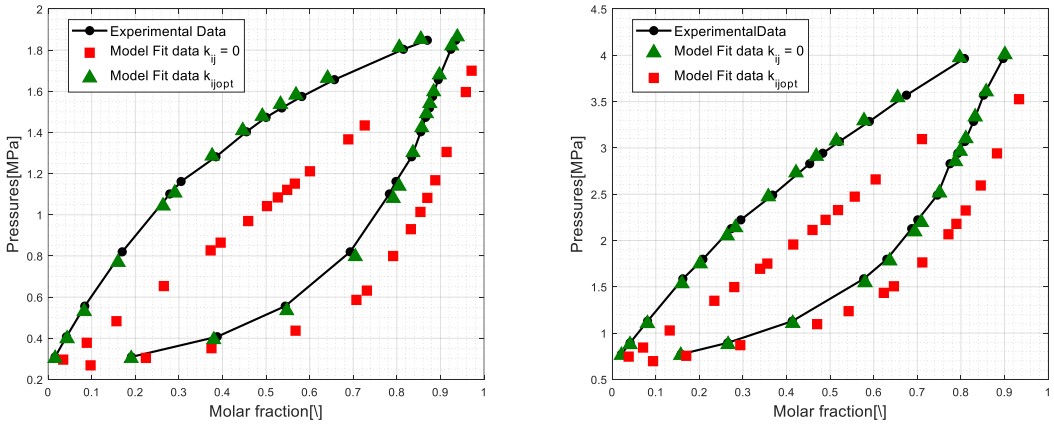

Figure 4.4 P-xy phase equilibrium diagram for a CO_2-Propane at 253.15 K and 283.15 K: solid line, liquid, and vapor composition experimental data; (Δ,▪) this study.

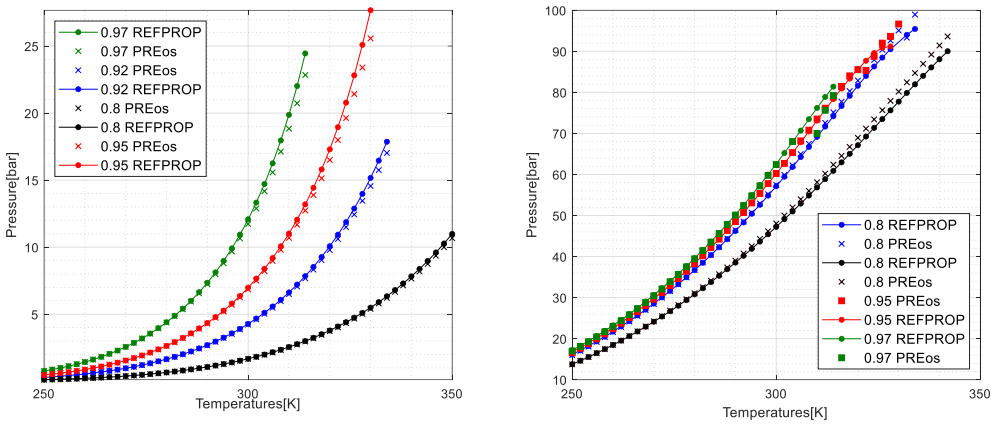

Figure 4.5 p-T phase equilibrium diagram for a CO_2-Acetone mixture at different composition: solid line, bubble, and dew pressure with REFPROP; (▪,ˣ) this study.

4.2 Departure functions and saturation curves: PR vs REFPROP

An approach based on the theory of departure functions coupled with the PR EoS adopted was used to calculate the thermodynamic properties of the mixture. For the application, the calculation has been restricted to the definition of enthalpy and entropy depicted the aim of the model. T-s, p-T, h-s diagrams were constructed for each mixture used. In this section, the purpose is to demonstrate how the model has been validated for a CO_2 – Acetone mixture by comparing calculated thermodynamic quantities with results obtained from REFPROP, and briefly describe the calibration methods and approaches used to compare the model constructed. To effectively validate the model, ensuring a coherent alignment not among the absolute or relative values of enthalpy and entropy, which, as any state function, depend on the chosen reference point, but among the residual quantities calculated at given (p, T). It is evident from the definition that a residual quantity is practically zero where real gases effects are not present, thus for conditions close to ideal gas, which means at much higher temperatures or at very low pressures compared to the critical point of the mixture. The delineation of these terms varies if the point is found under VLE condition or in a single-phase: in the first scenario, the residual quantity is weighted according to the mass vapor or liquid fraction of the mixture. A comparative analysis is provided for the mixture chosen, focusing on the residual quantities calculated utilizing PR EoS and delineated with the use of REFPROP by defining a temperature span across a series of isobars. Figure 4.6 shows the goodness of the model in defining the residual quantities for a given composition as the pressure varies.

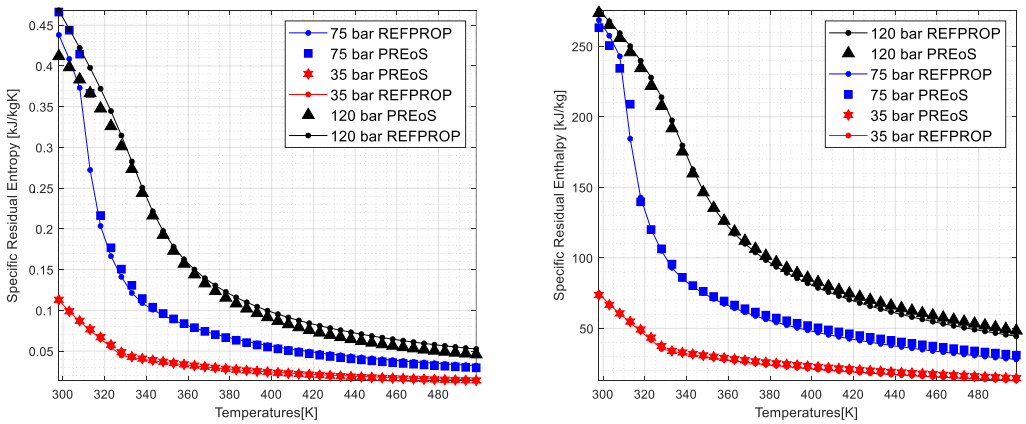

Figure 4.6 Residual functions against T for a CO_2-Acetone mixture for different pressures.

The results obtained are satisfactory in the superheated vapor region and at calculated points for subcooled liquid, with a slight deviation observed that is solely related to the residual calculation near very high vapor qualities where the PR recognizes fewer two-phase conditions. This can be observed also in Figure 4.7 where residual quantities are plotted for different composition on an isobar of 70 bar.

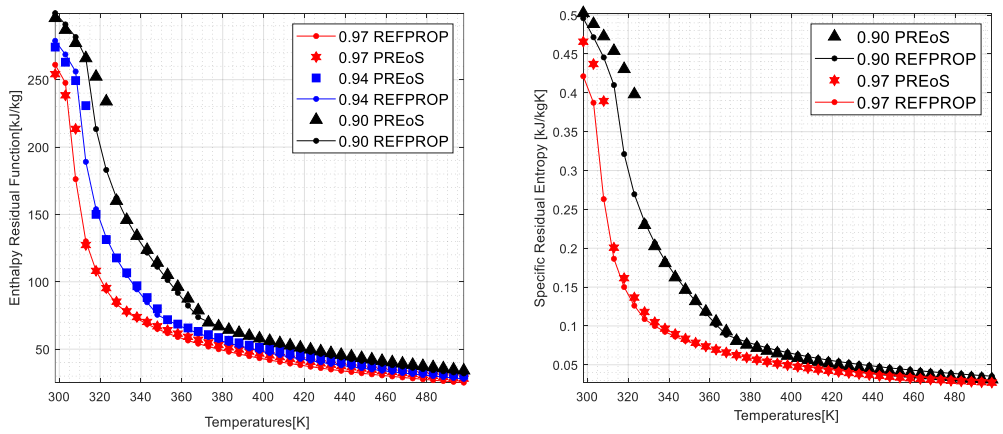

Figure 4.7 Residual functions against T for a CO_2-Acetone mixture for the same pressure for different compositions.

For completeness, the trends of the saturation curves are also compared in Figure 4.8. To model the curve's behaviour, BIP optimization is crucial before generating them, aiming for a better definition of the cricondenbar and cricondentherm . Generally, the accuracy of the EoS tends to be limited by calculations as the conditions are always close to critical conditions. The figures demonstrate, however, that the obtained results don't deviate excessively from REFPROP. A comparison is reported for two different compositions for the proposed mixture. This leads to observing how pressure-temperature points under saturation conditions are consistent.

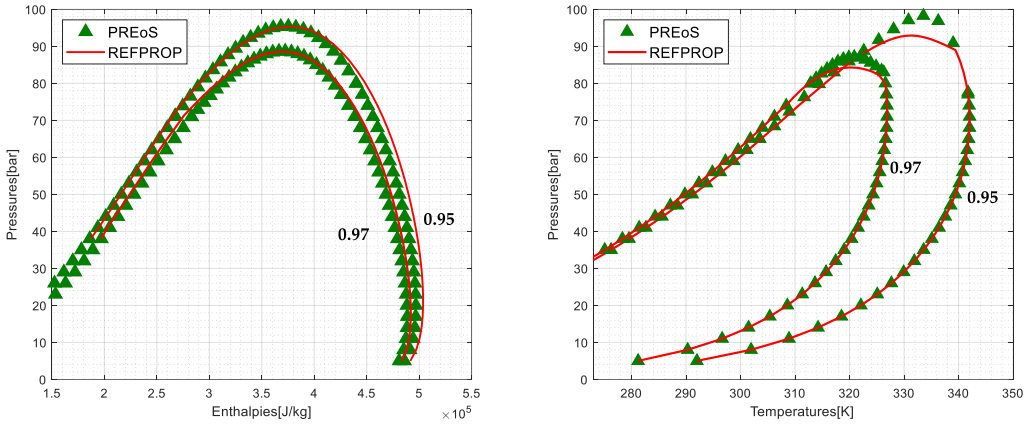

Figure 4.8 Comparing p-h, p-T diagrams for different compositions for a CO_2-Acetone mixture. (-) REFPROP, (Δ) this study.

5. Industrial high temperature applications

An overview analysis of a CO_2 - Acetone mixture is presented to observe its potentialities. Several case studies with large heat sink glides are presented to explore the effectiveness of the proposed mixture discussed by utilizing heatmaps. Analysing these cases helps to study different condition observing where high-temperature heat pumps with CO_2-based mixtures work best. As previously

said, tangible exergetic benefits are expected particularly when the source and sink require sensible heat exchange, so temperature glide at both becomes an important variable depending on the needs of industrial processes or the ΔT provided by the available low-temperature heat source. Some notable industrial applications where the introduction of HTHP could bring significant benefits refer to the production of *pressurized hot water production* (PHWP), where boilers can be substituted to make the heat delivery process more efficient [44]. Generalized cases reported of PHWP involve pressurized water heated from 140°C to 200°C. *Superheated steam drying* (SSD) is presented also as an innovative drying technology that uses superheated steam as a drying agent to eliminate excess water from a moist material. An advantage of this technology is that the exhaust from SSD is itself superheated steam, which can serve as a constant temperature waste heat source upon condensation. This heat is then upgraded by the HTHP through compression and used to increase the temperature of the superheated drying steam [28]. A particular process suggested by Bang-Möller [45] proposes SSD to dry wet biomasses, upgrading the temperature of vapor from 115 °C to 197 °C. A study proposed by Wang et al. [46] found that spray dryer inlet air is typically heated to 200°C or higher, with exhaust air temperatures ranging from 60–80°C and dew points of 35–40 °C. Simulations suggested 40% of the air heating load could be handled by HTHP, reducing energy costs by over 20%. Fully heating inlet air to 200°C using exhaust air alone is impractical due to large temperature lifts and a potential solution involves utilizing an external waste heat source with high energy content for direct heating. This case study is object of a detailed analysis discussed at the end of this section.

5.1 Results

The main operational parameters and plant assumptions for the reference case study are reported in Table 5.1, followed by the definition of the various cases for which a more in-depth analysis was conducted. Results are then reported for each case in the form of performance maps indicating the COP and second law efficiencies as a function of the inlet and outlet conditions of the heat sink.

$\eta_{is,compressor}[-]$	0.80	$T_{hot,source}[°C]$	75
$\eta_{is,expander}[-]$	0.80	$T_{in,rec}^{HOT}[°C]$	80:10:140
$\Delta T_{pp,rec}[°C]$	5	$\Delta p_{cond}[bar]$	1
$\Delta p_{eva}[bar]$	1	$\Delta p_{rec,cold}\|\Delta p_{rec,hot}[bar]$	0.5|1

Table 5.1 Operational parameters and sink/source assumptions.

- **Reference case**: CO_2 - Acetone mixture recuperative HTHP with expander, variable maximum pressure, waste heat source available at 75 °C. Pressure drops in the heat exchangers and turbomachinery efficiency are fixed.
- **Comparison with HTHP layout without expander**: analysis of the advantage achieved in COP for both recuperative and non-recuperative case.
- **Comparison with different waste heat sources available:** analysis on the possibility to use the same mixture at higher waste heat source temperature.
- **Reference not recuperative case**: analysis on the possibility to deliver sensible heat for heat sinks available at lower minimum temperatures without adopting a recuperative solution, but rather involving the use of the expander.

All mixture compositions are expressed on molar basis. Focusing on determining the optimal composition for the selected mixture, trends in COP, as well as glides obtained in the cooler and evaporator, are mapped. COP values are calculated while varying the compression ratio,

considering maximum achievable pressures that ensure controlled compressor temperatures. The maximum pressure set for the study is 250 bar, with maximum compressor outlet temperatures compressor of 240°C. To provide a more comprehensive analysis, various scenarios involving waste heat sources available at different temperatures are considered, along with different temperatures of the mixture exiting from the main heat sink, ranging from 80 to 140°C, to assess a wider range of applications. Furthermore, the thermodynamic analysis is limited to evaluating the performance of the heat pump, and therefore all temperatures are referenced to the CO_2 mixture. The ideal coupling, which also includes a techno-economic analysis and thus a design of the heat exchangers, is not investigated.

5.1.1 Reference Case

Results of the reference case are presented and discussed. An initial screening, not reported, led to a more detailed analysis of mixtures defined between 93% and 97% molar fraction of CO_2. Figure 5.1 depicts the trend of COP and η_{II} for a CO_2 - Acetone mixture with two different compositions. Different ranges in temperature are given by the range of pressures in which the study has been developed. For a 93% CO_2 – 7% Acetone mixture, considering trans-critical applications only, to is possible to work only at pressures next to the critical one, leading to a very small operating temperature range, as depicted in Figure 5.2, where iso-lines of pressures are shown, demonstrating that, for the imposed pressure and temperature conditions, the pressures at which the maximum temperatures are reached are limited to lower ones.

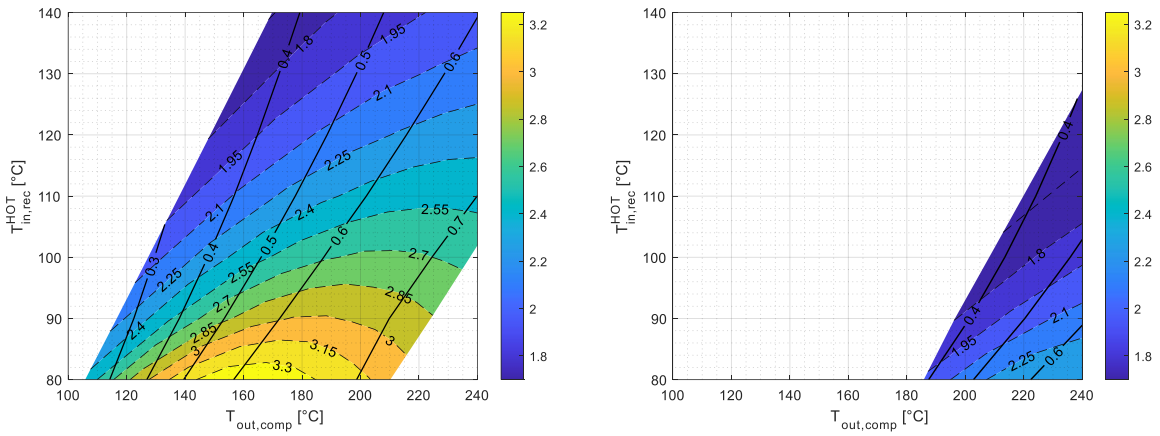

Figure 5.1 COP heatmaps for different compositions, with η_{II} iso-lines. On the left, for a 96% CO_2 – 4% Acetone mixture, on the right for a 93% CO_2 – 7% Acetone mixture.

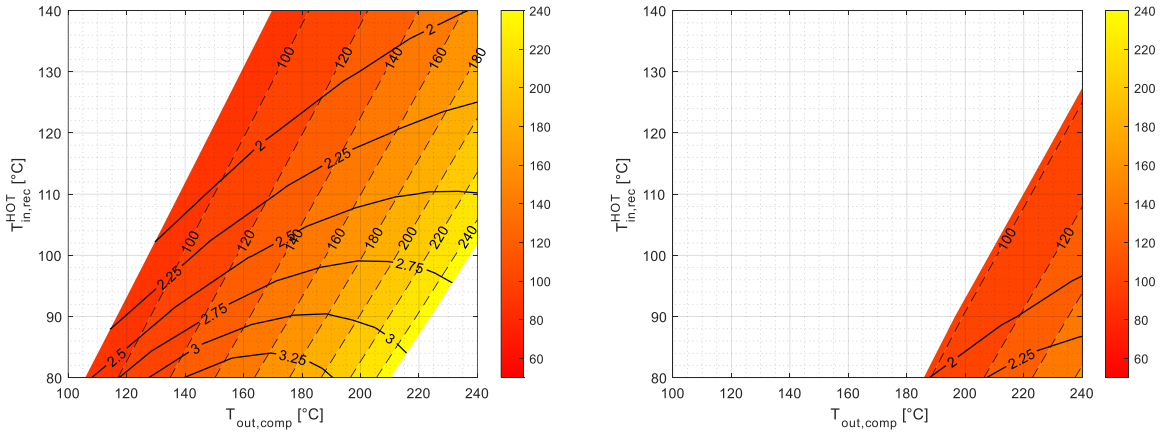

Figure 5.2 Pressures heatmaps for different compositions, with COP iso-lines. On the left, for a 96% CO_2 – 4% Acetone mixture, on the right for a 93% CO_2 – 7% Acetone mixture.

The maps show that for cases where the glide obtained at the cooler is high, the COPs obtained are promising for a 96% CO_2 – 4% Acetone mixture. As a result, as the cooler outlet temperature increases, COP will decrease, for the same compression ratio, due to the increase of the average heat rejection temperature in the cooler component. However, the iso-lines of η_{II} show how the heat supply can still be carried out efficiently, as the efficiency remains high. Therefore, supposing $T_{out,comp}$ constant, it is reasonable to expect that η_{II} decreases with the sink glide. Higher COP values are attained for lower minimum sink temperatures (for the reference case, the recuperator's minimum operating inlet hot side temperature is set at 80 °C). The effect of the expander, as will be pointed out later in the analysis, is approximately constant throughout the entire operating map. Moreover, the expander, does not ever produce a considerable effect such as to allow a good recovery, as described in the next section for a mixture at 93% molar fraction of CO_2.

In Figure 5.3 a heatmap is provided, depicting the maximum COP and the consequent second law efficiency for each operating condition within the range of analysed mixture compositions. The composition that maximizes the COP has been extracted. The map investigates, assuming $T_{out,comp}$ and $T_{in,rec}^{HOT}$ fixed, for which molar fraction of CO_2 the performance of the heat pump is maximized. Given the trend of the composition isolines, it is shown how the 96% CO_2 – 4% Acetone mixture, for the analysed conditions, seems to be the best within a wide operational range. It may be worth exploring the possibility of finding optimal solutions with mixtures at higher composition of CO_2. However, the reasons why they are of less interest are related to the lower COPs obtained and generally lower η_{II}. Furthermore, the operational conditions are highly restricted due to the maximum temperatures reached, with glide obtained in the evaporator which, in the majority of cases studied, are very low.

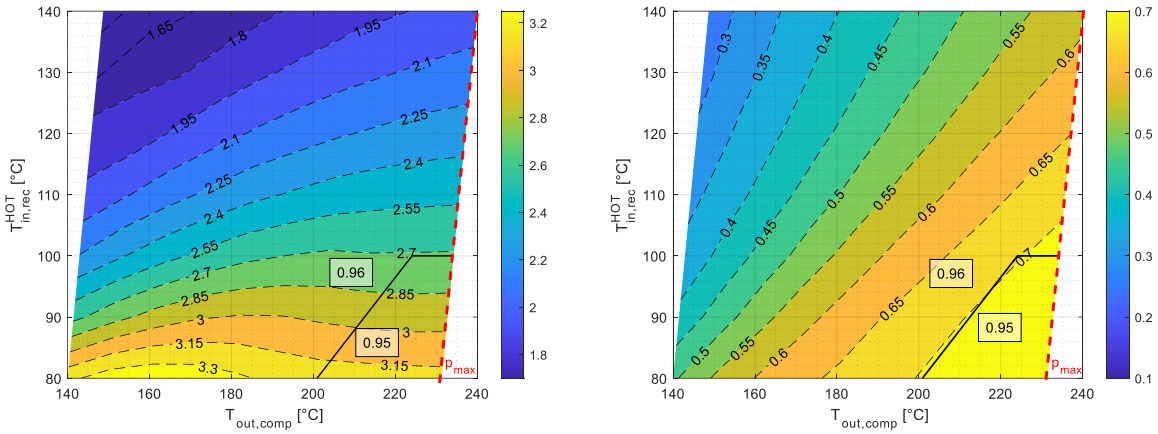

Figure 5.3 Maximum COP heatmaps and maximum η_{II} heatmaps for a variable mixture of 93-97% CO_2 – 7-4% Acetone, with optimal composition zones.

Specially for applications where the heat sink needs to be heated to high temperatures, the HP operates very efficiently. Figure 5.4 compares two different operating conditions, with the same compression ratio, for varying $T_{in,rec}^{HOT}$. Two configurations are observed with significantly different COPs, but with very high η_{II}. The provided ΔT_{sink} values are similar, but the average temperatures at which heat is supplied are different. Both heat sinks receive heat with good efficiencies, and part of the compression work is recovered by the expander. However, the recuperator exhibits pinch point difference temperatures which, in the case with the higher COP, are low both on the hot and cold sides.

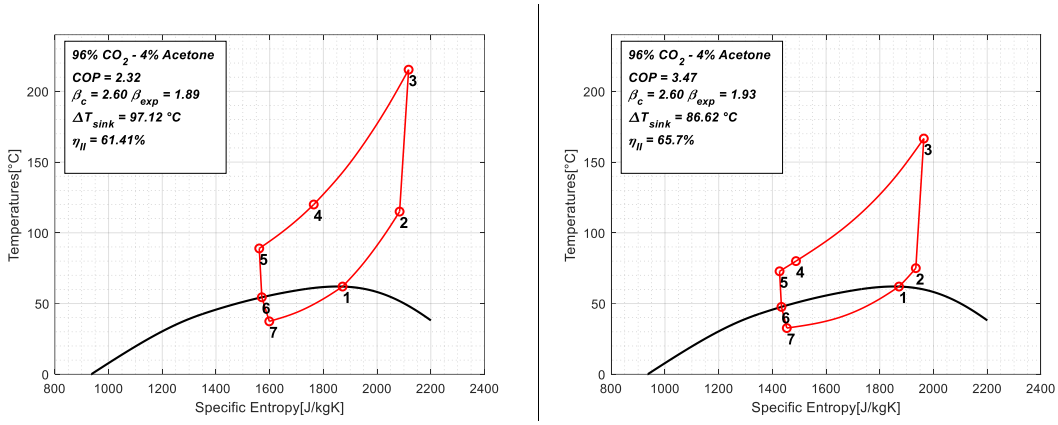

Figure 5.4 T-s diagrams for different HTHP configurations for a 96% CO_2– 4% Acetone mixture with $T_{max,source}$ = 75°C, same β_{comp}, for different $T_{in,rec}^{HOT}$.

Larger ΔT_{app} on the cold side are obtained if the $T_{in,rec}^{HOT}$ (T_4 in the Figure 5.4) is higher. The main cause is related to the different behavior of the c_p on the high-pressure and low-pressure sides of the recuperator. The slope of the isobar on the high-pressure side is lower, and consequently, T_5 is much higher than T_1. The effect is lower if the ΔT generated in the recuperator is minimal, and T_4 is close to T_1. Referring to Figure 5.4, higher COP in the region depicted can be attributed to two main reasons:

- At low T_4, fixed $\Delta T_{pp,rec}$ at the minimum design value, $\Delta T_{ap,rec}$ is lower. As a result, the thermal power exchanged with the sink is higher while keeping the compressor power consumption fixed.
- Higher maximum pressures result in greater work recovered by the expander, leading to a significant improvement in COP. Additionally, higher CO_2 content lowers p_{eva} enabling to adopt layout with a maximum temperature around 180÷220 °C and higher pressures. Consequently, the expander expansion ratio is higher and so the work recovered.

Another significant comparison illustrated in Figure 5.5, instead, depicts two T-s diagrams for different $T_{in,rec}^{HOT}$ (T_4 in the Figure 5.5), while maintaining $T_{out,comp}$ (T_3 in the Figure 5.5), constant. The compressor inlet temperatures vary significantly, and the lowest second law efficiencies are precisely associated with the lower temperature difference occurring in the high-pressure heat exchanger.

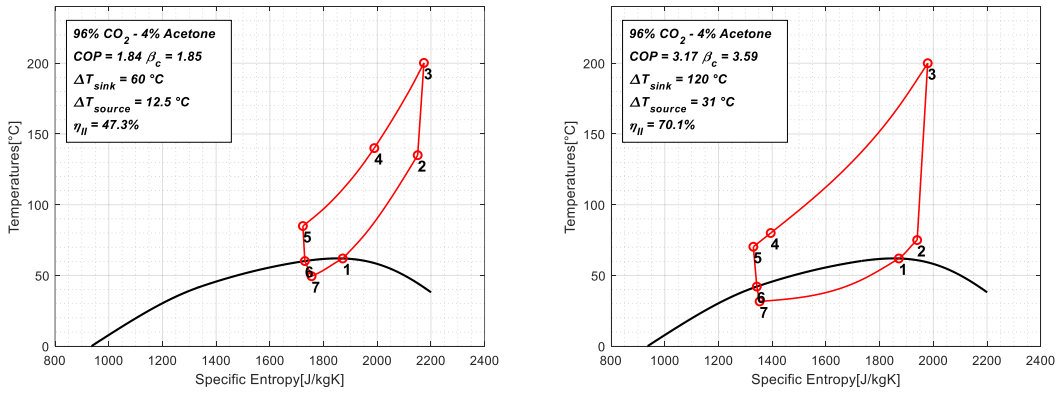

Figure 5.5 T-s diagrams for different HTHP configurations for a 96% CO_2– 4% Acetone mixture with $T_{max,source}$ = 75 °C, same $T_{out,comp}$, for different $T_{in,rec}^{HOT}$.

The advantage provided by the expander can be observed in Figure 5.6. T-s diagrams clearly show that for higher maximum pressures, expansion has a greater benefit on the mechanical power

consumed. A 17% power ratio between the expander and the compressor is noted as discussed later in the work. The composition that optimizes the COP exploits the advantages of the expander more effectively, highlighting that this technological solution, needs a more detailed analysis and consideration for cases where the obtained advantage is significant.

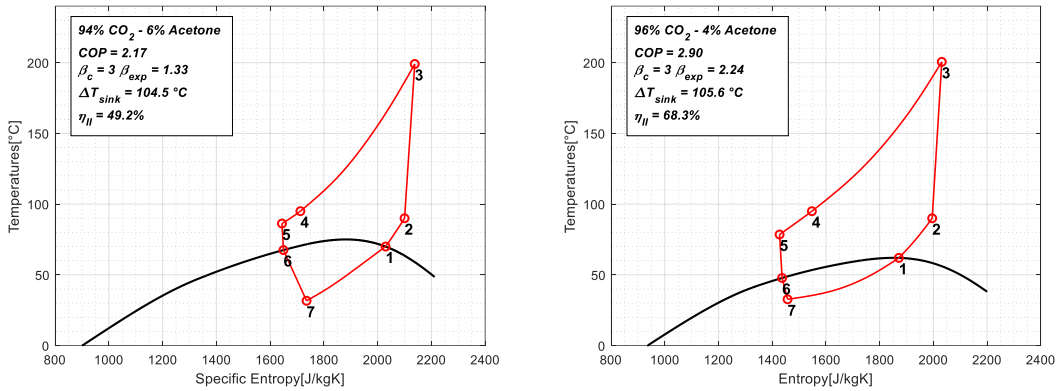

Figure 5.6 T-s diagrams for different HTHP configurations for a CO_2 – Acetone mixture for different compositions, with $T_{max,source}$ = 75 °C, same β_{comp}, same $T_{in,rec}^{HOT}$.

The temperature glide of both the sink and the source for the optimal mixture are depicted in Figure 5.7. Overall, the optimal mixture proposed provides large sink glides while effectively exploiting the waste heat source, especially for processes requiring heating from temperatures around 80-90 °C.

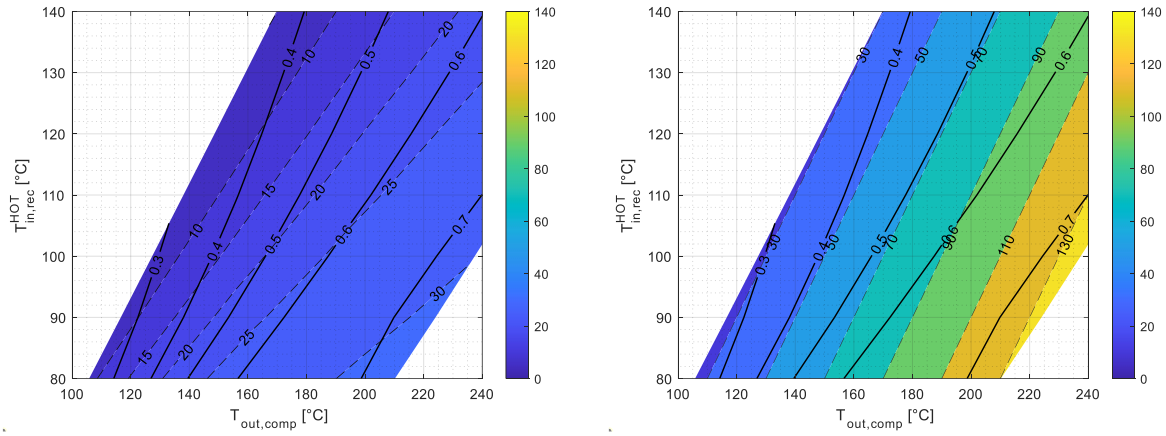

Figure 5.7 Heatmap of cold source glide on the left, heatmap of sink glide on the right, with COP isolines for a 96% CO_2 – 4% Acetone mixture on with $T_{max,source}$ = 70 °C.

For the application under study, with a waste heat source available at 75 °C, wherein the proposed mixtures are considered, high COP values are obtained for $T_{min,sink} = [80 - 100]\,°C$ and $T_{max,sink} = [170 - 220]\,°C$: where a high COP is achieved, the calculated η_{II} assumes promising values. Considering Equation 2, effective utilization of the low-grade waste heat source available allows for higher sink glide, defining better performances for a HTHP working with a 96% CO_2 – 4% Acetone mixture.

At least, in Figure 5.8 is presented a comparison of a p-h diagram obtained through REFPROP and the model provided in this thesis for an optimal case for a 95% CO_2 – 5% Acetone mixture.

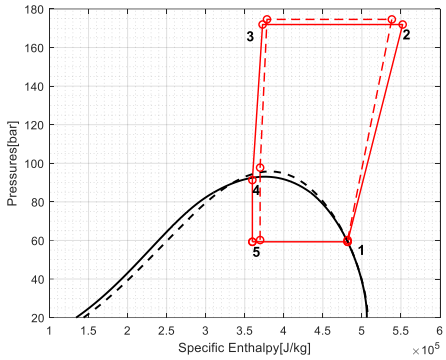

Figure 5.8 T-s diagram comparison for a 95% CO_2 – 10% Acetone mixture for a HTHP cycle with REFPROP (-), and PR model developed in this study (--).

REF|PR	T[°C]	p[bar]	COP	η_{II}[%]
1	68.5	59.3|60.2	3.17|3.33	58.6|59.7
2	169|163	172|175	β_{exp}	β_{comp}
3	85	172|175	1.88|1.80	2.9
4	55.3|58.1	91.3|97		
5	33.4|34	59.3|60.2		

Table 5.2 Comparison between the results obtained for a HTHP working with a 95% CO_2 – 10% Acetone mixture simulated both with REFPROP and the model developed in this study.

5.1.2 Comparison with HTHP layout without expander

In Figure 5.9, the comparison between the scenario with and without the expander reveals significant advantages in COP, averaging around 0.5 points where the COP is maximum. Advantages are particularly evident when the pressure difference in the expander has higher incidence with respect to the one through the valve. This point is consistent with previous results, highlighting the most substantial benefits in cases with compositions around 96% CO_2. In particular, it is observed that, for the same ΔT in the cooler, significant gains in second law efficiency are achieved with the expander, while maintaining the same trend of the COP iso-lines. In terms of COP itself, this translates to a considerable advantage on the performances, as observed in Figure 5.10.

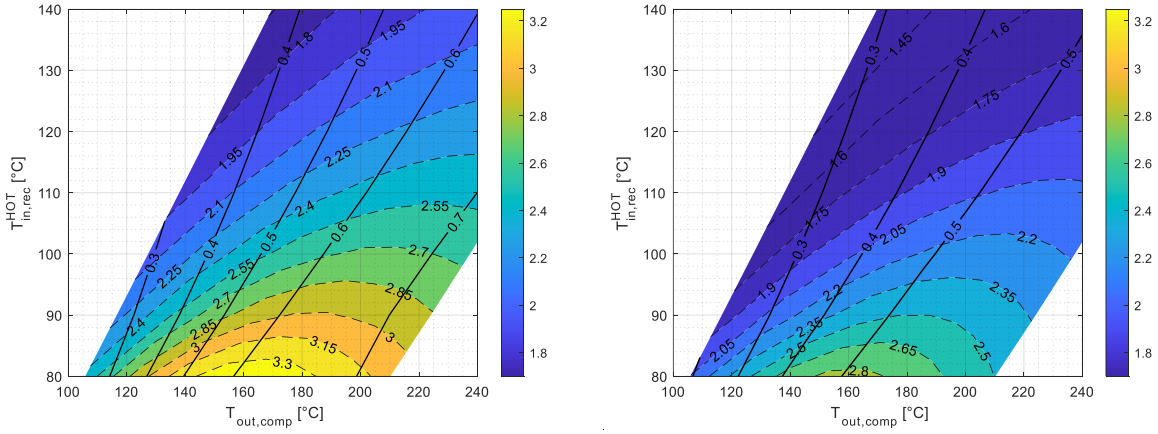

Figure 5.9 COP heatmaps for different compositions, with η_{II} iso-lines. On the left, for a 96% CO_2 – 4% Acetone mixture, on the right for a 93% CO_2 – 7% Acetone mixture.

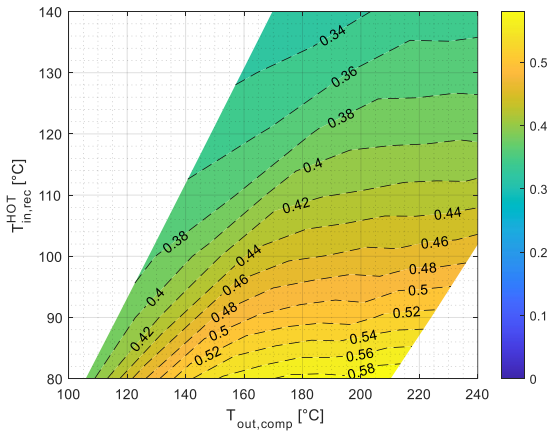

Figure 5.10 ΔCOP heatmaps between the reference case (i.e., recuperative with expander) and the one without expander for a 96% CO_2 – 4% Acetone mixture.

It is pointed out that the expander presents higher advantages for mixtures capable of reaching higher pressures while still maintaining limited outlet compressor temperatures. Specifically, the proposed 96% CO_2 – 4% Acetone mixture allows for a relatively low compression ratio given the available source, with significant expander recovery enabling a larger pressure variation compared to that achieved through the lamination. The analysed cases demonstrate promising potential for various high temperature industrial applications.

Furthermore, a defined HTHP layout under same operational conditions (i.e., same inlet and outlet cooler temperature, same heat source inlet temperature) shows how part of the difference in pressure can be carried out in the expander, avoiding all pressure discharge to be done through the valve, recovering part of the mechanical power expended for the compression. With the aid of Figure 5.12, this is shown for two configurations, showing the strong difference in performance. Additionally, with reference to Figure 5.11, for the case reported the ratio between the enthalpy drops of the expander and compressor is approximately 17.5%, underscoring the impact of the expander, thereby confirming what observed earlier.

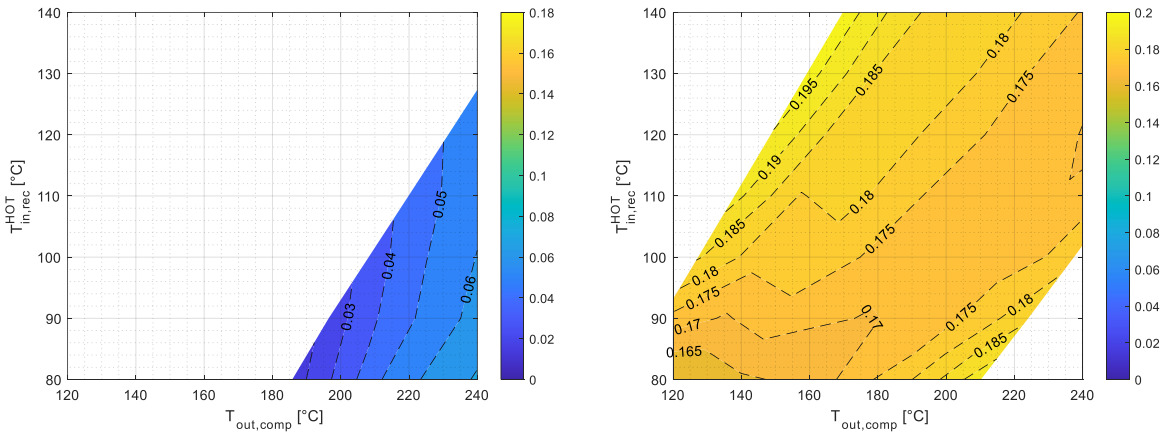

Figure 5.11 Ratio of the enthalpic drop of the expander against the enthalpic drop of the compressor heatmaps. On the left, for a 93% CO_2 – 7% Acetone mixture, on the right for a 96% CO_2 – 4% Acetone mixture.

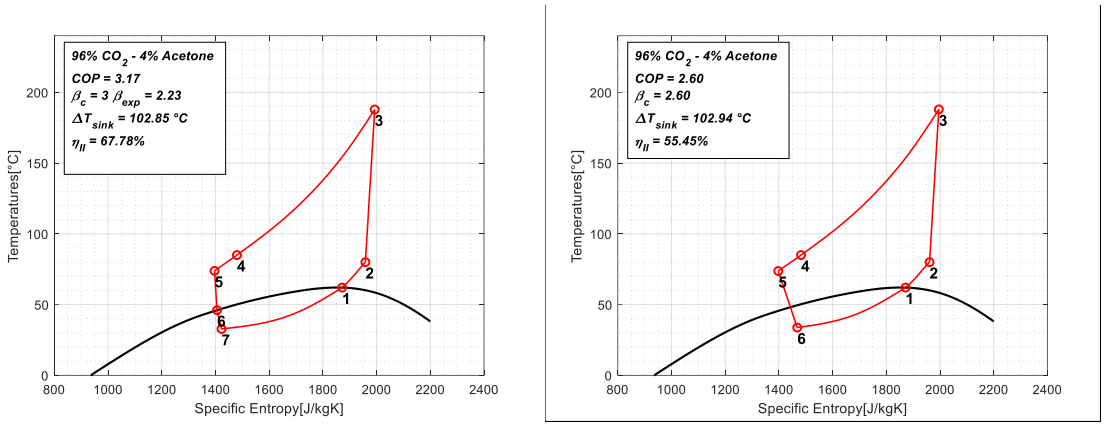

Figure 5.12 T-s diagrams for different HTHP configurations for a for a 96% CO_2 – 4% Acetone mixture with $T_{max,source}$ = 75 °C, same β_{comp}, $T_{in,rec}^{HOT}$. On the left, reference case layout. On the right, case without expander.

Figure 5.13 clearly demonstrates how the maximum COPs obtained without the use of the expander are significantly lower, observing how the utilization of a solution incorporating the expander allows to achieve maximum COPs with a lower variation in the mixture composition. Therefore, for a mixture of 96% molar fraction of CO_2, there exists a more stable range where the same composition optimizes the COP. Nevertheless, it is evident that cases where the CO_2 fraction is lower than the proposed one are not of interest if the source is available at the temperature fixed, highlighting how the optimization variables for a mixture are strongly variable, and the composition itself significantly impacts the maximum performance. Conversely, the η_{II} obtained under the same temperature differences are markedly lower if the expander is not present. This discrepancy is attributed to significantly higher second law losses in the valve and the regions where the COP get their maximum are shifted at lower maximum temperatures.

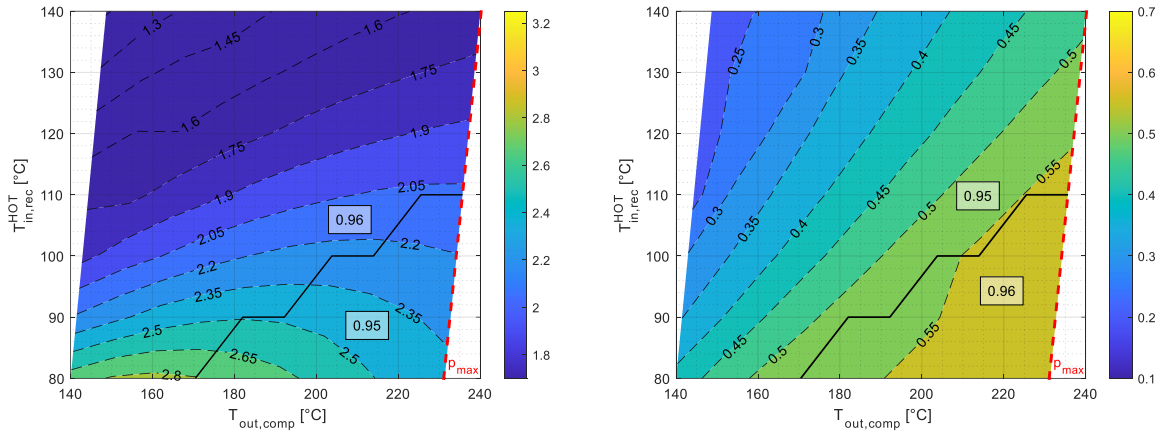

Figure 5.13 Maximum COP heatmaps and maximum η_{II} heatmaps for a variable mixture of 93-97% CO_2 – 7-4% Acetone, with optimal composition zones.

By the way, the temperature glide in the cooler remains unaffected by the adoption of a layout with or without an expander and similarly, the source glide exhibits minimal variation since the evaporator inlet temperature remains fairly constant in a large range of operating conditions, and the expansion process is isenthalpic.

5.1.3 Comparison with HTHP layout without recuperator

Adding a recuperator to the HTHP cycle, on average, results in higher COP, while pressure drops don't significantly affect the compression ratio. Increasing the inlet hot-side recuperator temperature, means to raise the compressor inlet temperature. Consequently, this leads to

compressor outlet temperatures that are too high, especially for mixtures with composition that allows to operate solely at pressures near the critical one (94% molar fraction of CO_2 - p_{crit} = 92.1 bar – p_{max} = 99 bar – $T_{min,sink}$ = 150 °C – $T_{out,comp}$ = 240 °C). Figure 5.14 shows HTHP COP and η_{II} in a non-recuperative asset for $T_{min,sink} = [40 - 80]\ °C$ both with expander and not for a 96% CO_2 - 4% Acetone mixture.

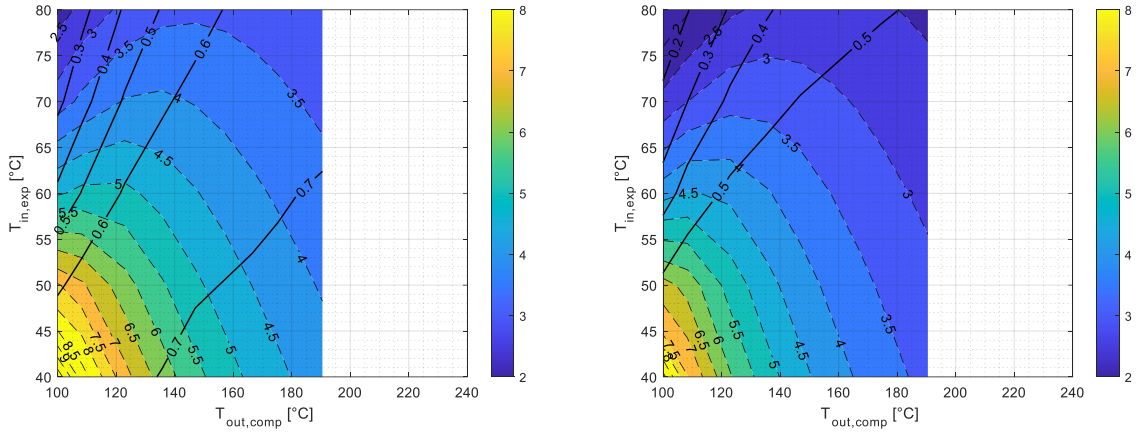

Figure 5.14 COP heatmaps with η_{II} iso-lines. On the left, for a 96% CO_2 – 4% Acetone mixture, on the right for a 93% CO_2 – 7% Acetone mixture.

It can be readily observed that the COP values are significantly higher if the temperature at which the mixture exits from the cooler is lower than the one of the waste heat source, but the maximum temperatures reached are lower, since they are constrained by compression ratios. To achieve higher $T_{out,comp}$, it would be necessary to push the cycle towards higher pressures. Therefore, a more comprehensive analysis will be required, given the more critical components that are needed in this kind of configuration. Additionally, it is interesting to observe through Figure 5.15 the ΔT done in the evaporator compared to that of the cooler: the attained glides are feasible, with a good COP achieved by effectively providing a high glide to the sink and with a good utilization factor of the heat source, approximately 30° over a wide range of cases.

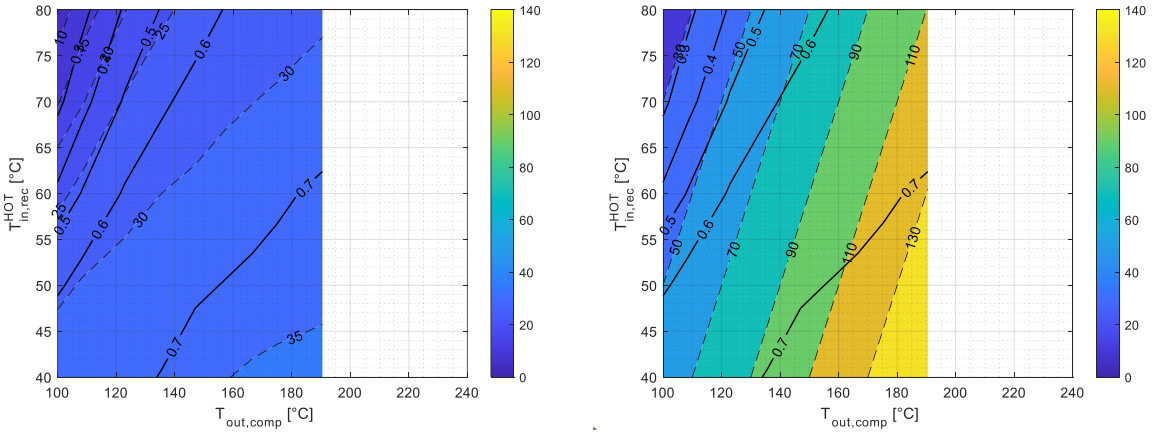

Figure 5.15 ΔT heatmaps for a 96% CO_2 – 4% Acetone mixture, with COP isolines. On the left, for ΔT_{eva}. On the right for ΔT_{cooler} .

Figure 5.16 shows how COPs are higher for inlet expander temperature below the compressor inlet one due to reduced temperature drop across the valve, minimizing irreversibilities. This solution shows great promise for industrial applications without requiring complex technological designs, with the expander offering noticeable advantages, thus working with a higher expansion ratio.

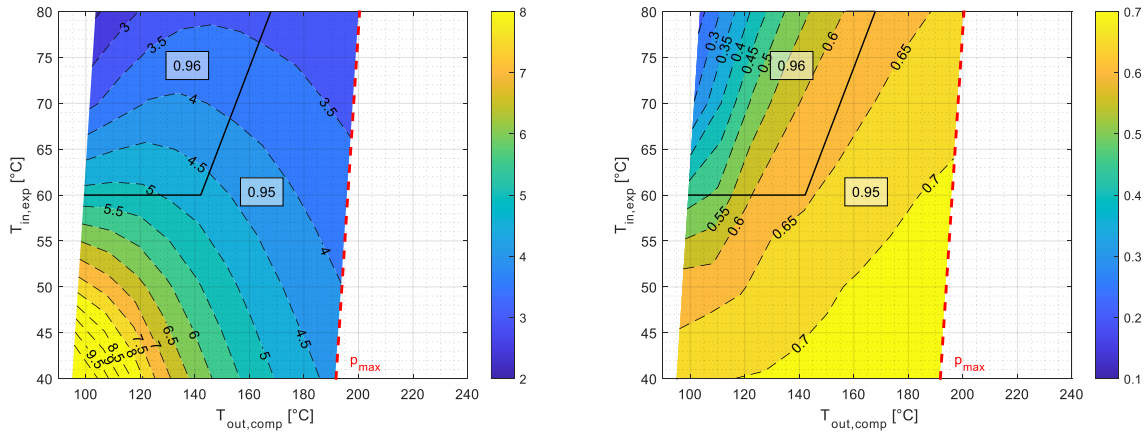

Figure 5.16 Maximum COP heatmaps and maximum η_{II} heatmaps for a variable mixture of 93-97% CO_2 – 7-4% Acetone, with optimal composition zones, for the HTHP layout with expander.

Unlike what was shown in the previous section, the composition that optimizes the COP changes for the cases now analyzed, where a 95% molar fraction of CO_2 ensures the best performance. Advantages obtained in terms of second-law efficiency are confirmed, and similarly, observing Figure 5.17, in the absence of the expander, for higher compressor outlet temperatures and lower cooler outlet temperatures, the optimal composition decreases.

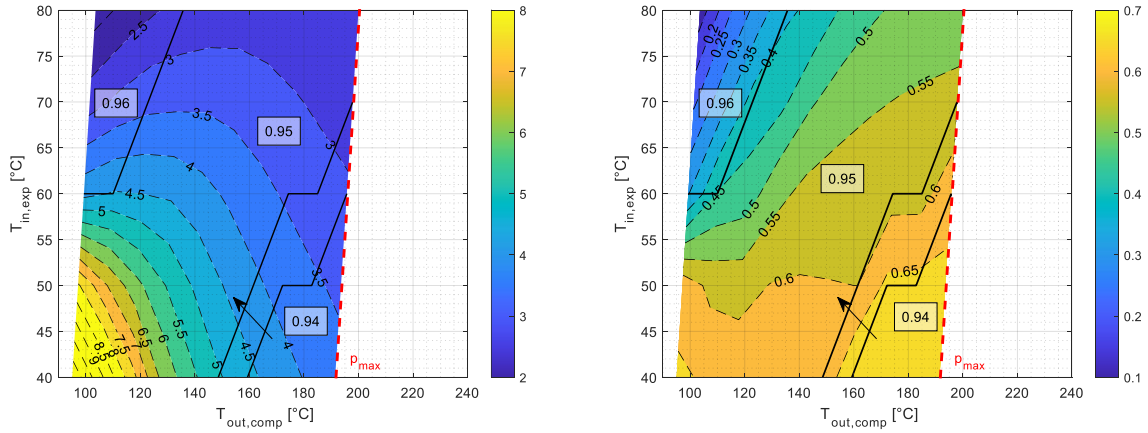

Figure 5.17 Maximum COP heatmaps and maximum η_{II} heatmaps for a variable mixture of 93-97% CO_2 – 7-4% Acetone, with optimal composition zones, for the HTHP layout without expander.

On the contrary, the real advantage of the recuperator lies in bringing the mixture to desired maximum temperatures [170-200 °C] at lower maximum pressures, while maintaining the same minimum pressure of the HTHP. Indeed, as reported in Figure 5.18, although the COPs without utilizing the recuperator are high, it is not possible to reach temperatures higher than 195°C without a steep increase in pressure, making the component design more critical and the application more limited. In conclusion, the recuperator allows for achieving higher heat pump efficiency while operating at lower maximum pressures, ensuring the same maximum cycle temperatures and COP, but with lower β_{comp}. However, it is possible to achieve a high sink glide even at lower average temperatures, with higher COPs in a non-recuperative setup.

The different trend in pressures can be explained by considering that in a non-recuperative configuration, as the cooler outlet temperature varies, the outlet compressor temperature depends only on the compression ratio and not on the inlet temperature, which is fixed. Conversely, in recuperative cases, the energy balance at the recuperator implies a variation in the inlet compressor

temperature. The different trend of the maps, therefore, in recuperative and non-recuperative configurations, is mainly related to the compressor outlet temperatures. At the same cooling end temperature, the recuperator allows for higher $T_{out,comp}$, because, at the same β_{comp}, $T_{in,comp}$ increases. Hence the diagonal trend of the maps for results for systems that exhibit recuperative configurations.

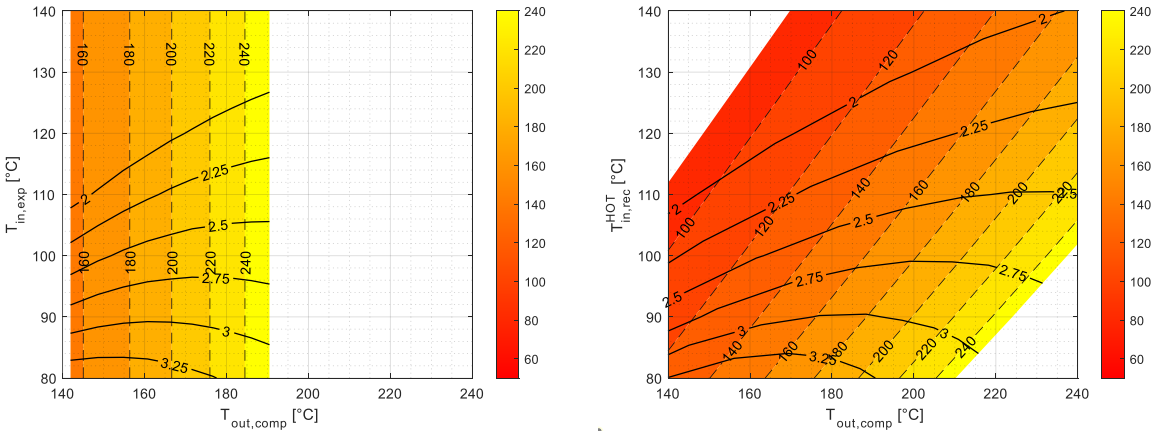

Figure 5.18 Maximum pressures comparison for a 96% CO_2 – 4% Acetone mixture. On the left, reference case layout (i.e., recuperative with expander). On the right not recuperative reference case layout.

5.1.4 Comparison with different waste heat available

Cases presented demonstrates how COP for a HP which works with a mixture significantly relies on various factors, particularly $T_{in,comp}$ which is intricately linked to the temperature at which of the low-grade waste heat source is available. Also, it depends on the specific design parameters of the evaporator. Moreover, the composition of the mixture introduces additional constraints but also more possibilities. The saturation curve and so the critical properties of the mixture change with its composition, presenting the possibility that the saturated vapor at the evaporator outlet might not be at a temperature higher enough to guarantee a good heat exchange with the source. Consequently, the COP is inherently tied to both the composition of the mixture and the characteristics of the available waste heat source. As a result, the obtained COP exhibits a strong dependency on the composition and a comprehensive analysis of different fluids could be beneficial in defining several optimal mixtures for different working conditions. From the study presented, as illustrated, even a slight variation in the dopant quantity leads to significantly change in performance. For the proposed 96% CO_2- 4% Acetone mixture, it is observed that saturated vapor enters the compressor with a maximum temperature of 62 °C. This implies that when dealing with waste heat sources available at higher temperatures, there would be increased irreversibilities in the evaporator, leading to less efficient utilization of the heat source. Being the critical temperature of Acetone higher than the one of CO_2, higher the quantity of Acetone in the mixture, higher the critical temperature. Therefore, a possible analysis can be developed by examining mixtures moved towards Acetone and studying their performance, while a second one involves changing mixture dopant. If the low-temperature waste heat source is available at higher temperature, it can be exploited in a recuperative HTHP to raise the thermal level of the mixture, providing heat to a sink that requires sensible heat at higher temperatures.

Considering a waste heat source available at 100°C, is investigated, under same $T_{out,comp}$ and $T_{in,rec}^{HOT}$, the composition which provide most efficiently the ΔT_{sink} for an industrial process which require sensible heat between 200°C and 110 °C. As the saturation curve varies, the three chosen

compositions (i.e., 88% - 90% - 92% CO_2 in molar fraction) have different critical temperatures. With a slight variation in the amount of dopant, the minimum pressures also vary.

A pinch point temperature of at least 5°C between the hot source and the mixture exiting the evaporator is considered. In particular, mixtures with compositions of 90% and 92% are such that they have saturated vapor exiting the evaporator at their cricondentherm . In Figure 5.19 are reported T-s diagrams for the condition proposed.

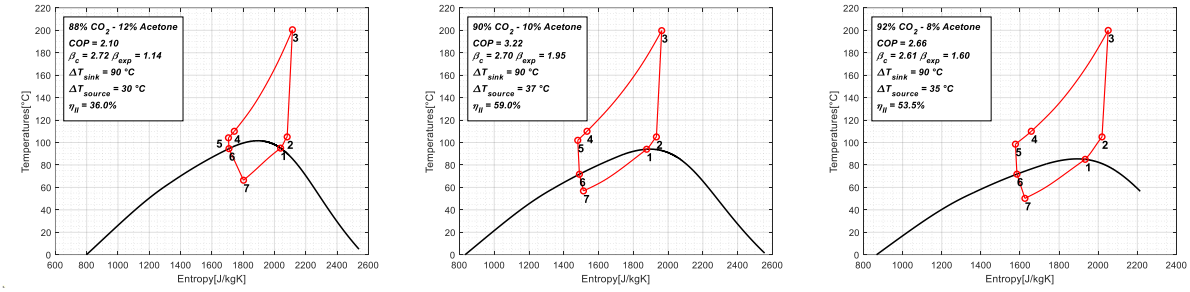

Figure 5.19 T-s diagrams for different HTHP configurations for a for a variable CO_2–Acetone mixture with $T_{max,source}$ = 100 °C, same $T_{in,rec}^{HOT}$ same $T_{out,comp}$.

What can be highlighted from the results is that the composition of the mixture that optimizes the COP is such the one that produces saturated vapor at a temperature equal to that at the cricondentherm , while still ensuring a low pinch at the end of the heat exchanger. The cricondentherm increases as the molar fraction of Acetone increases, and in the three cases studied, the mixture which have 90% of CO_2 molar fraction, has saturated vapor exiting the evaporator at 94°C. On the other hand, the mixture studied with the lower molar fraction of CO_2 operates not in proximity to the cricondentherm , constrained by the set pinch point with respect to the $T_{max,source}$. What has been shown is also consistent with the results obtained in the previous section. For a source available at 75 °C, a 96% CO_2 – 4% Acetone mixture has saturated vapor at the cricondentherm, optimizing heat exchange in the evaporator.

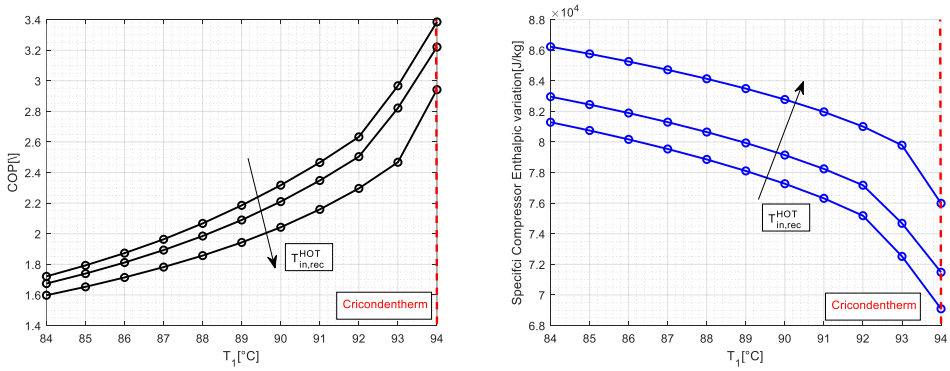

Figure 5.20 COP and specific compressor enthalpy variation trends with $T_{out,eva}$(T_1 in the figure), for different $T_{in,rec}^{HOT}$ (105 – 110 -120 °C), at same β_{comp}.

Additionally, higher COP under these conditions is also related to the fact that having saturated vapor to compress in these conditions, with higher density and higher compressibility factor, allows for optimal compressor power expended.

For the mixture which provide the best performance, in Figure 5.20 is indeed shown the variation of the COP and the enthalpy variation of the compressor with respect to $T_{out,eva}$ (T_1 in Figure 5.19) . It demonstrates how the enthalpy variation in the compressor is lower if the temperature is equal to the cricondentherm.

5.2 Case Study: Spray Drying with external heat source

The results obtained for the spray drying with external heat source case study are here reported. Information about the heat source and heat sink for the case are reported in Table 5.2. The aim of the case study is to assess the performance variation between a mixture and two pure fluids (Propane, R1233zd(E)) for different utilization factors of the heat source. Utilizing a mixture allows for a temperature glide during the evaporation phase, enhancing a good match between the source's cooling and the fluid's heating, with lower irreversibilities. As previously outlined, dry air is heated from 95°C to 200°C through a HTHP which exploits a water loop available at 100°C. To perform the analysis, a minimum outlet temperature of the heat source equal to 30°C is considered. The available heat source mass flowrate is 1.5 kg/s, which produces 441 kW of thermal power at the evaporator under maximum cooling conditions. This implies that if the source exits at a higher temperature, the exchanged power will be lower, and consequently, the power required by the compressor or the power delivered to the air will also be lower, while still ensuring the correct ΔT_{sink} required.

Heat Source		*Heat Sink*	
$T_{in}[°C]$	$T_{out}[°C]$	$T_{in}[°C]$	$T_{out}[°C]$
100	30:10:70	95	200

Table 5.3 Information about the heat source and the heat sink for the spray drying case study [47].

The technical constraints outlined in the chapter are respected, and the system exhibits only lower pressure losses in the evaporator (see Table 5.1). Specifically, the CO_2 - Acetone mixture tends to operate at higher pressures to provide the correct ΔT_{sink} to the air, whereas pure fluids operate at lower pressures under trans-critical conditions, at higher volume ratios. Figures 5.21-5.22 shows the comparison for the COP, volume ratio, $\dot{Q}_{sink}$ and the power expended for compression and recovered by the expander for different minimum temperature of the source.

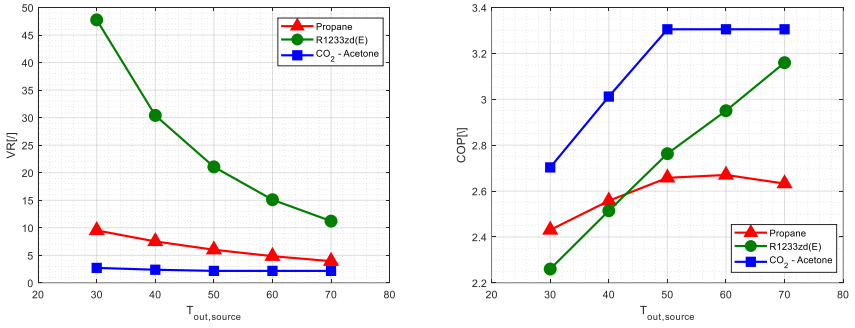

Figure 5.21 COP, VR comparison for a CO_2 - Acetone mixture, Propane, R1233zdE.

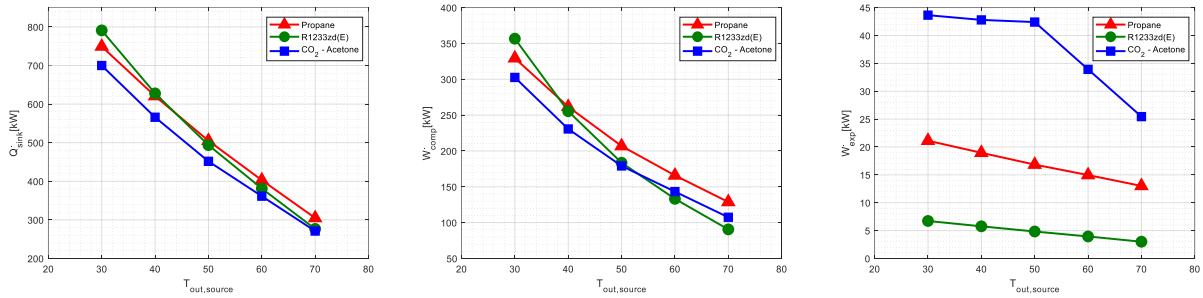

Figure 5.22 $\dot{Q}_{sink}$, $\dot{W}_{comp}$, $\dot{W}_{exp}$ comparison for a CO_2 - Acetone mixture, Propane, R1233zdE.

The results demonstrate that the mixture consistently performs better than both Propane and R1233zd(E) in terms of COP varying the utilization factor of the heat source. Propane shows a

marginal increase in COP, while R1233zd(E) exhibits a significant boost, achieving a COP of 3.16 compared to the mixture's 3.30 for $T_{out,source} = 70\ °C$. This COP plateau observed with the mixture is attributed to two main reasons: despite the higher outlet temperature of the heat source, a CO_2 – Acetone mixture maintain the inlet evaporator temperature roughly constant to 45 °C resulting in a high COP even with a larger ΔT_{app} at the cold side of the evaporator compared to pure fluids, which achieve optimal COPs with a 5°C pinch point. Moreover, similar COPs are got for the same β_{comp} and $T_{out,comp}$, as the mixture exits the evaporator at a temperature equal to its cricondentherm, for a ΔT_{source} = [30-50] °C.

Furthermore, when subjected to compression, mixtures allow for significantly lower volume ratios compared to pure fluids. With increasing COP, the VR decreases for all three studied fluids. Despite the higher maximum pressures reached for the mixture in the proposed cases, the volume ratio is significantly lower, with an average value around 2.5. It emerges so that the volume ratio at the compressor does not vary significantly for the mixture with the variation of the source's utilization, a trend completely different from that observed for R1233zd(E). The number of stages in the compressor is generally defined based on the total enthalpy drop produced or on the volume ratio. Depending on the complexity of the fluid, a design criterion is generally preferred, and given that blade loading is usually restricted for high molecular mass working fluids, as is the case here, control over the VR is preferred. It is also noted how lower VRs of the mixtures allows for simpler design and lower operating costs, adopting solutions with fewer stages. Therefore, despite the generally lower operating pressures for the pure fluid, the compressor design would be more critical and highly variable depending on how much the source is cooled. The power required for compression is significantly reduced for the mixture and additionally, the power ratio between the expander and compressor favors the CO_2 mixture. This implies that, at the same outlet temperature of the heat source (i.e., same $\dot{Q}_{source}$), a slightly lower delivered $\dot{Q}_{sink}$ is obtained. However, considering the significant smaller work required to compress the mixture, the COP is higher. Comparatively, R1233zd(E) requires less compression work for high outlet temperatures of the heat source with respect to the mixture, but the recovery in the expander is significantly lower, resulting in a lower COP.

6. Pumped Thermal Energy Storage (PTES) application

In this chapter, a concise overview of a PTES layout will be presented, with a focus on basic thermodynamics and adopted plant solutions. The discussion will then shift to describing the proposed and developed methodology for simulating the system, coupled with a case study. PTES is a highly promising and emerging technology in the field of large-scale energy storage. A heat pump operates by utilizing electrical energy to transfer heat from a low-temperature source to a high-temperature one in the charging phase. Subsequently, during the discharge phase, the heat stored is used to run the power cycle: this thermal storage unit delivers efficiently heat thus the stored thermal energy is converted back into electrical energy.

A fundamental criterion for evaluating the efficacy of any electrical energy storage technology is its RTE: generally, PTES system can be divided into Brayton PTES and Rankine PTES [48]. The Brayton PTES system typically exhibits a large operational temperature range spanning from -70 °C to 950 °C and RTEs within the range of 45% to 75% [49] [50]. Conversely, Rankine PTES operates at temperatures generally lower. Particularly, when functioning below 250°C, the round-trip efficiencies of both the organic Rankine PTES system, spanning from 23% to 48% [51], and the trans-critical CO2 Rankine PTES system, approximating 53% [52]. Furthermore, integrating low-grade

heat sources with the Rankine PTES system offers greater versatility due to their widespread availability. Examples include industrial waste heat, geothermal energy, and solar energy.

6.1 Overview of a conventional PTES configuration

As briefly introduced, an interesting approach to enhancing performance involves investigating appropriate system configuration of PTES with heat integration [53].

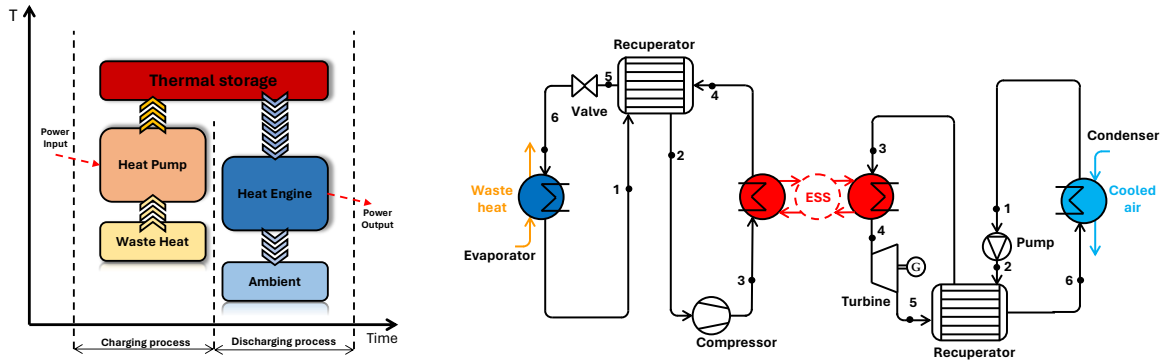

Figure 6.1 Schematic diagram of PTES system with Heat Integration and PTES layout at charging and discharging process.

This low-grade waste heat source is upgraded to a high-grade thermal energy during the charging process. The thermal energy produced is stored and in the discharge phase, the ESS releases heat energy, which is then utilized to power the heat engine, specifically an ORC, in response to the need for electricity generation [54]. Following the cycle in the Figure 6.1, during the charging of the storage the CO_2-based mixture is compressed reaching a maximum temperature which corresponds to a trans-critical or supercritical condition, entering then in a heat exchanger in which it is cooled transferring energy to the storage system, with low pressure drops.

Post thermal exchange, the mixture is expanded at low pressure through a throttling valve, to enter in an evaporator in which low-grade heat is absorbed, completing the cycle. For discharging the process is simply reversed. The organic fluid is pumped from low pressure to high pressure exchanging heat first in the recuperator and then from the storage in the primary heat exchanger, producing vapor which expands in an expander connected to a generator produce electric power. Mixture discharged goes through the recuperator and the condenser.

6.2 Thermal storage system (ESS)

One of the critical aspects of the trans-critical CO_2 PTES system is related to the storage efficiency, which depends on the matching of the hot storage system and the temperature profile of the high-pressure side of the charge cycle [52], where as a result of the real gas effects near the critical point, the temperature behavior exhibited becomes markedly nonlinear. Considering the need to ensure a good RTE, which would be penalized if solutions for storage were adopted don't allowing for a good match between charging and discharging, without going into a discussion on possible solutions already extensively studied in literature [55] [56], it's briefly described the possibility of a storage system based on solid media.

The principle of this approach involves storing heat during the charging phase by utilizing a solid medium to heat up CO_2 as it cools down. Subsequently, during the discharging phase, the solid medium is cooled to heat the working fluid before it enters the expander. This process completely decouples the temperature profiles of charging and discharging CO_2, allowing a crossing of curves in the TQ diagram with the aim to optimize temperature differences at both cold and hot sides. Two

primary architectures are commonly employed for this storage technology: packed bed and solid matrix solutions [57].

The first offers a significantly larger heat transfer area compared to the solid matrix configuration, given the same volume, with better performance, sharper thermoclines, and a more compact storage system with the limitation of being unable to maintain the same internal pressure and stronger mechanical stresses for certain plant configurations. On the contrary the solid matrix structure significantly reduces stresses as the fluid flows within pipes of smaller diameter, adopting a longer system, as the thermocline profile becomes flatter.

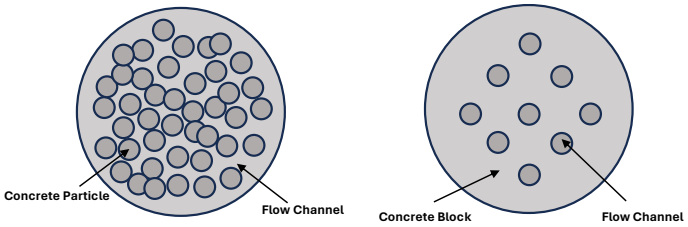

Figure 6.2 Solid energy storage structures. On the left, packed structure. On the right, solid matrix structure.

6.3 Thermodynamic Analysis

RTE stands as a fundamental parameter in evaluating the performance of PTES systems. It denotes the *Key Performance Indicator* (KPI) to evaluate the PTES effectiveness. A good RTE means superior efficiency in both the transfer and utilization of stored thermal energy, thus allowing higher system performances, thereby reducing the cost of the system.

$$RTE = COP_{heating} * \eta_{I,ORC} \tag{11}$$

For this purpose, the first law efficiency accounts for both the electrical and mechanical consumption of the expander and the pump.

$$\eta_{I,ORC} = \frac{(h_{in} - h_{out})_{turb} * \eta_{mech,el,turb} - \frac{(h_{out} - h_{in})_{pump}}{\eta_{mech,el,pump}}}{(h_{out} - h_{in})_{PHE}} \tag{12}$$

6.4 Discharge Methodology

The methodology employed to integrate the charging and discharging cycles is observed in Figure 6.3. While the proposed approach for the charging phase remains consistent with the one developed (see Section 2), a dedicated setup has been addressed for the numerical resolution of the ORC cycle. Considering the selected charging configuration, it resolves the constraints associated with storage and defines the requisite input variables for the discharging phase.

The solver extracts a comprehensive structure comprising all thermodynamic and performance results from the charging phase, important for delineating temperatures and the RTE. Subsequently, the discharging phase is solved. The extracted variables regard the maximum and minimum temperatures at which the working fluid enters in the storage, and the COP. Furthermore, a preliminary control scheme is established, aligning with the proposed layout for the HTHP to ensure precise temperature specifications. The resolution of the ORC cycle follows standardized procedures, with the designated input variables:

- **Ambient temperature and the condenser's approach point ΔT_{app},** from which is evaluated the condensation temperature T_{cond}. The condenser uses ambient air at 30°C, allowing the condensation of the discharge fluid.
- **Expansion ratio β_{exp},** to define how the RTE change with the maximum pressure of the discharge cycle.

Additionally, the recuperator is essential to cover the heat supply required, raising the discharge fluid to the inlet temperature of the storage, utilizing the steam generated by the turbine, which, if in superheated steam conditions, allows for a more efficient thermal recovery. Consequently, ensuring the energy balance at the recuperator becomes fundamental, with cases considered feasible only when, under the specified charging conditions, there are no crossovers in the temperature profiles within the recuperator.

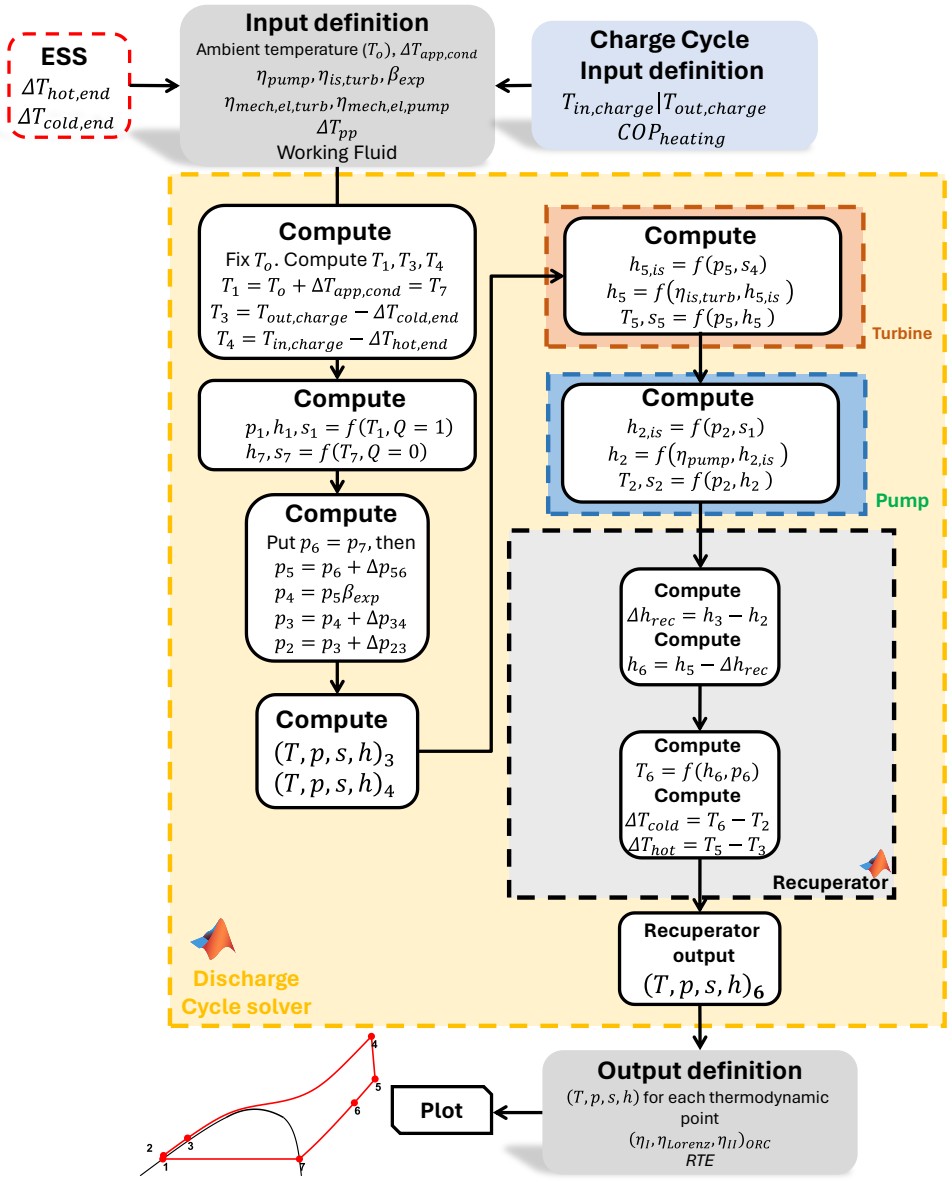

Figure 6.3 Numerical solving approach for the discharge cycle of PTES. ORC solver methodology.

6.5 Case Study: application to CO_2-based CSP plants

Case study refers to the use of rejected heat available from the *Heat Rejection Unit* (HRU) of a sCO_2 cycle of a *Concentrated Solar Plant* (CSP) for PTES. The charge fluid is a CO_2-Acetone mixture used in

the plant configuration upon which the proposed innovation of the thesis work is based. The discharge fluid, on the other hand, will be a pure fluid. The pressure losses and the mechanical and isentropic efficiencies used for the ORC are reported in Table 6.1, while the low-temperature heat source of the HP proposed to be used is a close-loop of demineralized water heated in the HRU of the power cycle of the CSP plant, with the perfect characteristics to be the heat source of the HP. Operational parameters for the charge cycle are presented in the previous chapter (see Table 5.1). Demineralized water is available from the cycle HRU at 75°C, which can be cooled down in a temperature range around 40-44°C [58], exploited from two different proposed HTHP configurations.

$\eta_{is,pump}[-]$	0.80	$T_{hot,source}[°C]$	75
$\eta_{is,turbine}[-]$	0.85	$\Delta p_{eva}[bar]$	1
$\eta_{mech-el,turbine}[-]$	0.98	$\Delta p_{cond}[bar]$	1
$\eta_{mech-el,pump}[-]$	0.98	$\Delta p_{rec,cold} \mid \Delta p_{rec,hot}[bar]$	0.5 | 0.5
$\Delta T_{storage,hot}[°C]$	5	$\Delta T_{storage,cold}[°C]$	5
$\Delta T_{app,cond}[°C]$	15	$T_o[°C]$	25

Table 6.1 ORC Operational parameters for PTES application,

The reported case study aims to assess whether a HTHP utilizing a CO_2 – Acetone mixture may ensure high RTEs, when coupled with a suitable discharge fluid, while exploiting the close-loop of demineralized water available. Main layout results of the two configurations chosen for the charge cycle are reported below in Table 6.2.

LAYOUT A				LAYOUT B			
$\Delta T_{source}[°C]$	39	$T_{max,charge}[°C]$	122.5	$\Delta T_{source}[°C]$	39	$T_{max,charge}[°C]$	188
$\Delta T_{sink}[°C]$	70	$COP[-]$	6.0	$\Delta T_{sink}[°C]$	108	$COP[-]$	3.2

Table 6.2 Operational parameters for the charge cycle.

Given RTE definition, from a thermodynamic point of view very high RTEs could be achieved for very low temperature lift in the heat pump, exaggerating the effect of the temperature difference between heat pump source and power cycle heat sink. A purely thermodynamic analysis diverges from what can be the optimization from a technical-economic point. COPs considerably high means to have large exchange areas and more critical designs, implying efficient heat transfer but challenges in managing large thermal loads. Similarly, a lower ORC η_I, takes challenges due to high mass and volumetric flows, necessitating large heat exchangers. This leads to increase to complex design, potentially impacting on the operational cost of the plant. As the effect of heat introduction leads to an expected increase in RTE for low *Turbine Inlet Temperatures* (TITs), following the trend of the ideal efficiency for both COP and cycle efficiency according to Equation 11, the two configurations aim to explore then how the η_I of the ORC and consequently the RTE are affected by the maximum temperature of the HP. Both cases use the same discharge fluid, pure Propane, whose properties are obtained from the REFPROP database, chosen because its critical conditions match well with the thermodynamic conditions of the charge configuration chosen, suitable for investigating trans-critical applications.

Layout A demonstrates that RTE is promising. The COP of the heat pump is indeed very high but working at low TIT results in very penalizing efficiencies for the ORC. On the contrary, Layout B shows how, in this case study, pushing the design towards ORC optimization, working at lower COPs for the heat pump, results in lower RTEs, but from a technical-economic standpoint, certainly more feasible.

LAYOUT A				LAYOUT B			
η_I	10.8%	RTE	65.2%	η_I	17.8%	RTE	56-5%

Table 6.3 Results obtained for PTES.

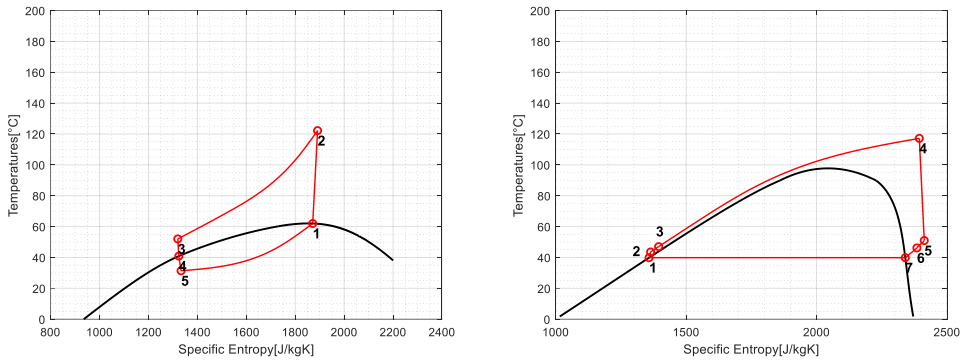

Figure 6.4 T-s diagram for the charge and discharge cycle of the PTES Layout A.

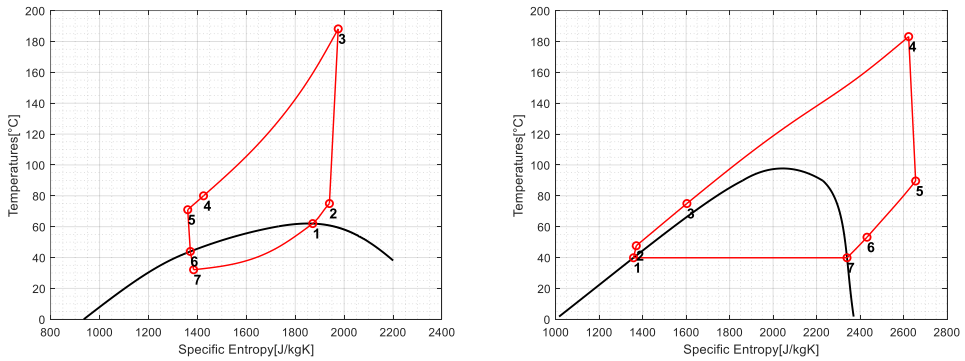

Figure 6.5 T-s diagram for the charge and discharge cycle of the PTES Layout B.

Furthermore, considering the results obtained, it is advantageous, for achieving higher RTEs, to push the design towards HTHP with very high COPs. In particular, non-recuperative cases, studied in the previous chapter, with a minimum sink temperature lower than the evaporator outlet temperature, present COPs in the range of 4.5-8. Considering the necessity of completely cool down the waste heat source, the range of possible optimal configurations for HTHP is certainly limited. Similarly, HTHP operating with higher COPs also operate at lower average temperatures. This implies that the power cycle will have lower efficiencies, being highly dependent on TIT and on the average temperature at which power is delivered. As briefly mentioned, Layout A appears to be thermodynamically optimal but less realistic from a techno-economic perspective due to critical design requirements for both the HP and ORC. COP variability under operational conditions using a fluid mixture is also challenging. Conversely, Layout B appears significantly more realistic and feasible, while maintaining reasonable thermodynamic efficiencies. In this layout, the HTHP operates in recuperative mode, and the expander allows operation with a stable mixture composition over a wide operational range, enabling storage with high efficiency without excessively penalizing the ORC's performance.

The condensation temperature also greatly influences RTE. The lower the condensation pressure, the greater the increase in RTE at the same TIT. Reducing p_{cond}, acting on the $\Delta T_{app,cond}$,while maintaining a constant expansion ratio, enhances efficiency improving thermodynamic performance and work produced by the turbine. However, for the application proposed, condensation temperatures are typically maintained around 40°C, while ambient temperatures range from 25-30°C.

7. Conclusion and future developments

In this thesis, the modelling of CO_2-based mixture HTHP has been analysed. The study focused on analysing HTHP performance identifying which are the main parameters that affect the COP, investigating possible applications for industrial processes that require heat at higher temperatures (180-240°C). One of the main challenges of HTHPs is the integrability into the production process industry and to match the available heat source to the required heat demand. CO_2-based mixture (i.e., CO_2- Acetone mixture) are investigated as working fluid for HTHP, exploring the potential use of CO_2 which can also derive from carbon capture and storage processes. Mixtures allows temperature glide during evaporation and condensation, matching better the temperature glide of the heat source and sink, reducing irreversibilities. Furthermore, to recover part of the mechanical power expended for compressing the working fluid, to higher pressures (up to 250 bar), a promising technological solution involving an expander is proposed. The numerical model for thermodynamic resolution was implemented in MATLAB, exploiting the capabilities of REFPROP V10.

After presenting the system architecture in its new technological proposal and the numerical model, it was also considered to develop a numerical model that would define the thermodynamic conditions of fluids and mixtures based on the PR EoS. As strongly emphasized, this allows to study any type of mixture and calibrate a model based on experimental data collected from literature. The model was also tested for the development of thermodynamic calculations for the numerical resolution of HPs. The HTHP performance analysis results, presented in the form of heatmaps, underscore the efficacy of using mixtures as working fluids to obtain elevated COP under specific operational conditions. Two case studies, one for HTHP and one for PTES, are presented for the investigated technologies.

The results underscore the efficacy of using mixtures as working fluids to obtain elevated COP under specific operational condition. A thermodynamic analysis reveals that integrating an expander into the system significantly enhances the COP and η_{II}. Additionally, little variations in mixture composition or cycle minimum temperatures yield substantial performance variations, introducing challenges such as the need for precise composition control, but at the same significant versatility for various heat source characteristics. This versatility proves particularly advantageous in complex industrial applications where the thermal utilization of waste heat sources is required to decarbonize several heating processes. Specifically, mixtures at 96% of CO_2 exhibit approximately 0.5 points of COP advantage over configurations without the expander, with work recovery equal roughly to the 18% of compressor work. Optimal performances are achieved when exploiting heat sources available at temperatures similar to the mixture's cricondertherm, as compressed vapor density increase, allowing for lower mechanical work to compress it. Furthermore, pressure reduction done in part by the expander is particularly efficient when the inlet pressures are significant, as in the case of HTHP based on CO_2 mixtures. The use of a CO_2 - Acetone mixture to heat air up to a temperature of 200°C has shown that, compared to the two proposed pure fluids, the obtained COPs are higher. With the same glide produced by the source, the energy spent to compress the mixture is lower, but more importantly, the mechanical power recovered in the

expander is significantly higher. Additionally, the compressor design appears to be less critical, despite the higher operating pressures, given the significantly lower and relatively constant volume ratios with varying effective utilization of the source.

For PTES scenarios, employing mixtures operating in trans-critical conditions allows better match with the thermal energy storage, as well as an efficient exploitation of the heat source available, demineralized water (from 75°C to 40-45°C) with the charge mixture proposed, characterized by a typical 30-40°C temperature glide along evaporation.

Future research could utilize these results for further exploration of the technology. A techno-economic optimization analysis could be conducted to effectively assess whether the proposed solutions are technically effective. Regarding the PR Eos model, new developments for mixtures not specifically used in this study are proposed.

References

[1] P. Kokic, S. Crimp and M. Howden, "A probabilistic analysis of human influence on recent record global mean temperature changes," *https://doi.org/10.1016/j.crm.2014.03.002*, 2014.

[2] I. Jebabli, A. Lahiani and S. Mefteh-Wali, "Quantile connectedness between CO2 emissions and economic growth in G7 countries," *https://doi.org/10.1016/j.resourpol.2023.103348*, 2023.

[3] Y. Xu, H. Zhang, Y. Wu and o. , "Performance of compressed air energy storage system under parallel operation mode of pneumatic motor," *https://doi.org/10.1016/j.renene.2022.09.133*, 2022.

[4] S. Impram and o. , "Challenges of renewable energy penetration on power system flexibility: A survey.," *https://doi.org/10.1016/j.esr.2020.100539*, 2020.

[5] N. A. Sepulveda, "Decarbonization of Power Systems: Analyzing Different Technological Pathways," *Department of Nuclear Science and Engineering & Institute for Data, Systems, and Society*, 2016.

[6] K. Xiaoxue, W. Ruzhu and o. , "Heat pump assists in energy transition: Challenges and approaches," *https://doi.org/10.1016/j.decarb.2023.100033*, 2024.

[7] W.-D. Steinmann, D. Bauer, J. Henning and J. Maike, "Pumped thermal energy storage (PTES) as smart sector-coupling technology for heat and electricity," *https://doi.org/10.1016/j.energy.2019.06.058*, 2019.

[8] A. Benato and A. Stoppato, "Pumped Thermal Electricity Storage: A technology overview," *https://doi.org/10.1016/j.tsep.2018.01.017*, 2018.

[9] A. K. Vuppaladadiyam, E. Antunes and others, "Progress in the development and use of refrigerants and unintended environmental consequences," *https://doi.org/10.1016/j.scitotenv.2022.153670*, 2022.

[10] P. Neksa, "CO2 heat pump systems," *https://doi.org/10.1016/S0140-7007(01)00033-0*, 2000.

[11] A. Carro, R. Chacartegui and others, "Energy storage system based on transcritical CO2 cycles and geological storage," *https://doi.org/10.1016/j.applthermaleng.2021.116813.*

[12] G. Manzolini, M. B. D. Binotti, C. Invernizzi and I. P., "CO2 mixtures as innovative working fluid in power cycles applied to solar plants. Techno-economic assessment," *https://doi.org/10.1016/j.solener.2019.01.015.*

[13] J. Gómez-Hernández, R. Grimes, J. Briongos, C. Marugán-Cruz and D. Santana, "Carbon dioxide and acetone mixtures as refrigerants for industry heat pumps to supply temperature in the range 150–220 °C.," *https://doi.org/10.1016/j.energy.2023.126821.*

[14] "NIST Reference Fluid Thermodynamic and Transport Properties Database (REFPROP): Version 10," *https://www.nist.gov/srd/refprop.*

[15] S. Quoilin, M. Van Den Broek and others, "Techno-economic survey of organic rankine cycle (ORC) systems," *https://doi.org/10.1016/j.rser.2013.01.028*, 2013.

[16] S. Lecompte, H. Huisseune and a. , "Review of organic Rankine cycle (ORC) architectures for waste heat recovery," *https://doi.org/10.1016/j.rser.2015.03.089.*, 2015.

[17] J.Bao and L. Zhao, "A review of working fluid and expander selections for organic Rankine cycle," *https://doi.org/10.1016/j.rser.2013.03.040*, 2013.

[18] C. Arpagaus, F. Bless and others, "High temperature heat pumps: Market overview, state of the art, research status, refrigerants, and application potentials," *https://doi.org/10.1016/j.energy.2018.03.166*, 2018.

[19] K. Chua and others, "Advances in heat pump systems: A review," *https://doi.org/10.1016/j.apenergy.2010.06.014*, 2010.

[20] J. Jiang, B. Hu, R. Wang, N. Deng, F. Cao and C.-C. Wang, "A review and perspective on industry high-temperature heat pumps," *https://doi.org/10.1016/j.rser.2022.112106*, 2022.

[21] D. Wu, b. Hu and al., "Vapor compression heat pumps with pure Low-GWP refrigerants".

[22] C. Magni, R. Peeters, S. Quoilin and A. Alessia, "Assessing the Flexibility Potential of Industrial Heat–Electricity Sector Coupling through High-Temperature Heat Pumps: The Case Study of Belgium," *https://doi.org/10.3390/en17020541*, 2024.

[23] J. Gomez-Hernandez, R. Grimes and others, "Carbon dioxide and acetone mixtures as refrigerants for industry heat pumps to supply temperature in the range 150–220 o," *https://doi.org/10.1016/j.energy.2023.126821*, 2023.

[24] R. Moreira-Da-Silva, S. D. and A. Coronas, "Modelling of CO2/acetone fluid mixture thermodynamic properties for compression/resorption refrigeration systems," *10.1088/1757-899X/595/1/012030.*

[25] G. Frate, L. Ferrari and U. Desideri, "Analysis of suitability ranges of high temperature heat pump working fluids," *https://doi.org/10.1016/j.applthermaleng.2019.01.034*, 2019.

[26] W. Nyemba, S. Chinguwa, B. Marango and C. Mbohwa, "Evaluation and feasibility assessment of the sustainability of refrigeration systems devoid of harmful refrigerants for storage of vaccines," *https://doi.org/10.1016/j.promfg.2019.05.042.*

[27] F.-M. Adrián, M.-B. Adrián, G.-P. Pau and N.-E. Joaquín, "Optimal refrigerant mixture in single-stage high-temperature heat pumps based on a multiparameter evaluation," *https://doi.org/10.1016/j.seta.2022.101989.*

[28] H. Abedini, E. Vieren, T. Demeester, W. Beyne, S. Lecompte, S. Quoilin and A. Arteconi, "A comprehensive analysis of binary mixtures as working fluid in high temperature heat pumps," *https://doi.org/10.1016/j.enconman.2022.116652.*

[29] S. Shoujun, G. Hao, L. Ding, B. Yin and G. Maoqiong, "Performance of a single-stage recuperative high-temperature air source heat pump," *https://doi.org/10.1016/j.applthermaleng.2021.116969,* 2021.

[30] Z. Yang, L. Huanwei and X. Wu, "Theoretical and experimental study of the inhibition and inert effect of HFC125, HFC227ea and HFC13I1 on the flammability of HFC32," *https://doi.org/10.1016/j.psep.2011.09.009,* 2012.

[31] G. Ferrara, L. Ferrari, D. Fiaschi, G. Galoppi and o. , "A small power recovery expander for heat pump COP improvement," *https://doi.org/10.1016/j.egypro.2015.12.140.*

[32] S. Singh, M. Dasgupta and A. Singh, "CFD Modeling of a Scroll Work Recovery Expander for Trans-critical CO2 Refrigeration System," *https://doi.org/10.1016/j.egypro.2017.03.081,* 2017.

[33] S. Singh, M. Dasgupta and A. Singh, "CFD Modeling of a Scroll Work Recovery Expander for Trans-critical CO2 Refrigeration System," *https://doi.org/10.1016/j.egypro.2017.03.081,* 2017.

[34] D. Roskosch, V. Venzik, J. Schilling, A. Bardow and B. Atakan, "Beyond Temperature Glide: The Compressor is Key to Realizing Benefits of Zeotropic Mixtures in Heat Pumps," *https://doi.org/10.1002/ente.202000955,* 2021.

[35] T. Ommen, W. Meesenburg, B. Elmegaard and others, "Generalized COP estimation of heat pump processes for operation off the design point," *10.18462/iir.icr.2019.0648.*

[36] A. Bejan and M. Moran, "Thermal design and optimization," *10.1016/S0140-7007(97)87632-3.*

[37] D. Peng and D. Robinson, "A new two-constant equation of state," *Ind. Eng. Chem. Fundam.*, 1976.

[38] A. Martín, M. D. Bermejo, M. F. A. and M. J. Cocero, "Teaching advanced equations of state in applied thermodynamics courses using open source programs," *https://doi.org/10.1016/j.ece.2011.08.003,* 2011.

[39] "NASA Glenn Coefficients for Calculating Thermodynamic Properties of Individual species".

[40] M. J. Assael, T. J. P. M. and T. F. Tsolakis, Thermophysical Properties of Fluids.

[41] C. Chonghui, Z. Naijun and others, "A prediction model for the binary interaction parameter of PR-VDW to predict thermo-physical properties of CO2 mixtures".*https://doi.org/10.1016/j.fluid.2022.113634.*

[42] E. Gisselle, Y. Zgar and others, "Vapor-liquid equilibrium, liquid density and excess enthalpy of the carbon dioxide+acetone mixture: Experimental measurements and correlations," *https://doi.org/10.1016/j.fluid.2020.112915,* 2021.

[43] M. Stavrou, A. Bardow and G. J., "Estimation of the binary interaction parameter kij of the PC-SAFT Equation of State based on pure component parameters using a QSPR method," *https://doi.org/10.1016/j.fluid.2015.12.016.*

[44] C. Mateu-Royo, A. Mota-Babiloni and o. , "Advanced high temperature heat pump configurations using low GWP refrigerants for industrial waste heat recovery: A comprehensive study," *https://doi.org/10.1016/j.enconman.2020.113752,* 2021.

[45] C. Bang-Møller, M. Rokni and o. , "Decentralized combined heat and power production by two-stage biomass gasification and solid oxide fuel cells," *https://doi.org/10.1016/j.energy.2013.06.046,* 2013.

[46] J. Wang, C. Brown and others, " Heat pump heat recovery options for food industry dryers," *https://doi.org/10.1016/j.msea.2018.03.037,* 2018.

[47] E. Vieren, T. Deemester and others, "The thermodynamic potential of high-temperature transcritical heat pump cycles for industrial processes with large temperature glides," *https://doi.org/10.1016/j.applthermaleng.2023.121197,* 2023.

[48] O. Dumont, G. Frate, A. Pillai, S. Lecompte, D. P. M. and V. Lemort, "Carnot battery technology: A state-of-the-art review," *10.1016/J.EST.2020.101756.*

[49] T. Liang, A. Vecchi and others, "Key components for Carnot Battery: Technology review, technical barriers and selection criteria," *https://doi.org/10.1016/j.rser.2022.112478.*

[50] A. Benato and A. Stoppato, "Heat transfer fluid and material selection for an innovative Pumped Thermal Electricity Storage system," *https://doi.org/10.1016/j.energy.2018.01.045.*

[51] D. Venzik, V. Atakan and others, "Potential analysis of pumped heat electricity storages regarding thermodynamic efficiency," *10.1016/J.RENENE.2018.09.023,* 2018.

[52] M. Mercangoz, J. Hemrle, L. Kaufmann and A. O. C. Graggen, "Electrothermal energy storage with transcritical CO2 cycles," *Energy 2012;45:407–15.*

[53] K. Ökten and B. Kurşun, "Thermo-economic assessment of a thermally integrated pumped thermal energy storage (TI-PTES) system combined with an absorption refrigeration cycle driven by low-grade heat source," *https://doi.org/10.1016/j.est.2022.104486,* 2022.

[54] Z. Meiyan, S. Lingfeng, S. Gequn and others, "Configuration mapping of thermally integrated pumped thermal energy storage system," *https://doi.org/10.1016/j.enconman.2023.117561.*

[55] M. Morandin, "Conceptual Design of a thermo-electrical Energy Storage System Based on Heat Integration of Thermodynamic Cycles – Part A: Methodology and Base Case," *10.1016/j.energy.2012.03.031*, 2012.

[56] M. Morandin, "Conceptual Design of a thermo-electrical Energy Storage System Based on Heat Integration of Thermodynamic Cycles – Part B: Alternative System Configurations," *10.1016/j.energy.2012.03.033*, 2012.

[57] W. Ming and others, "The Impact of Concrete Structure on the Thermal Performance of the dual-media Thermocline Thermal Storage Tank Using Concrete as the Solid Medium," *10.1016/j.apenergy.2013.08.044*, 2014.

[58] M. Doninelli, E. Morosini, G. Gentile, L. Putelli, G. B. M. Di Marcoberardino and G. Manzolini, "Thermal desalination from rejected heat of power cycles working with CO2-based working fluids in CSP application: A focus on the MED technology," *https://doi.org/10.1016/j.seta.2023.103481*, 2023.

Appendix

Peng-Robinson Equation

Peng-Robinson Equation is a two-parameter Equation of State cubic in volume, with all parameters expressible in terms of critical pressure p_c, critical temperature T_c, and acentric factor ω.

$$p = \frac{RT}{V-b} - \frac{a(T)}{V(V+b)+b(V-b)} \tag{13}$$

For each component of the mixture, the following relation are valid:

$$a(T_c) = \frac{0.45725R^2}{p_c}T_C \quad b(T_c) = \frac{0.07780R}{p_c}T_C \quad a(T) = a(T_c)\alpha(T_r.\omega) \tag{14}$$

$$\alpha^{0.5} = 1 + (1 - T_r^{0.5})(0.37464 + 1.5422\omega - 0.26992\omega^2) = (1 - T_r^{0.5})n \tag{15}$$

$$A = \frac{0.45724\alpha p_r}{T_r^2} \quad B = \frac{0.07780}{T_r}p_r \quad D = na(\alpha T_r)^{0.5} \tag{16}$$

For mixture, combining rules are used to mutual describe the interaction between components.

$$a\alpha = \sum\sum x_i x_j (a\alpha)_{ij} \quad b = \sum\sum x_i x_j b_{ij} \quad (a\alpha)_{ij} = (1 - k_{ij})(\left((a\alpha)_i (a\alpha)_j\right)^{0.5} \tag{17}$$

$$a_{ij} = \left(1 - k_{ij}\right)\left(a_i a_j\right)^{0.5} \; b_{ij} = \frac{(b_i + b_j)}{2} \tag{18}$$

$$A_{mix} = \frac{a\alpha p}{(RT)^2} \quad B_{mix} = \frac{bp}{RT} \tag{19}$$

Then fugacity coefficients of both phases are then obtained, once computed the compressibility factor:

$$z^3 - (1 - B)z^2 + (A - 3B^2 - 2B)z - (AB - B^2 - B^3) = 0 \tag{20}$$

Residual quantities

Residual quantities are computed to define the deviation from ideal conditions to real ones for a fluid in any region of the thermodynamic plane. Given the formulation adopted for c_p^o (see Equation 7), then ideal enthalpy and entropy are reported.

$$\frac{H^o(T)}{RT} = -a_1 T^{-2} + \frac{a_2 lnT}{T} + a_3 + \frac{a_4 T}{2} + \frac{a_5 T^2}{3} + \frac{a_6 T^3}{4} + \frac{a_7 T^4}{5} + \frac{b_1}{T} \tag{21}$$

$$\frac{S^o(T)}{R} = -\frac{a_1 T^{-2}}{2} - a_2 T^{-1} + a_3 lnT + a_4 T + \frac{a_5 T^2}{2} + \frac{a_6 T^3}{3} + \frac{a_7 T^4}{4} + b_2 \tag{22}$$

The residual quantities of enthalpy and entropy are then computed, defined mixtures coefficient.

$$\frac{S^R(T)}{R} = \ln[Z - B] - \frac{BD}{2.828a\alpha A}\ln\left(\frac{z + 2.414B}{z - 0.414B}\right) \tag{23}$$

$$\frac{H^R(T)}{RT} = 1 - z + \left(\frac{A}{2.828B}\right)\left(1 + \frac{D}{a\alpha}\right)\ln\left(\frac{z + 2.414B}{z - 0.414B}\right) \tag{24}$$

For residual computation in 2-phase condition, overall specific extensive property is weighted on two sub-part on their respective molar fraction (or mass fraction γ if the specific quantities are on mass). Using NIST, the precise formulations adopted are the following:

$$\Delta h(T, p, z_i) = (1 - \gamma)\Delta h(T, p, x_i)_{bubble} + \gamma \Delta h(T, p, y_i)_{dew} \tag{25}$$

$$\Delta \mathrm{s}(T, p, z_i) = (1 - \gamma)\Delta \mathrm{s}(T, p, x_i)_{bubble} + \gamma \Delta s(T, p, y_i)_{dew} \tag{26}$$

Abstract in lingua italiana

Relatore:
Prof. Dario Alfani

Correlatore:
Ettore Morosini

Anno accademico:
2023-24

In risposta all'urgente necessità di soluzioni energetiche sostenibili, le pompe di calore ad alta temperatura e i sistemi PTES rappresentano rispettivamente tecnologie promettenti per i processi di riscaldamento industriale e lo stoccaggio dell'energia su larga scala. Il lavoro di tesi esplora il potenziale delle miscele a base di CO_2 come fluido di lavoro per pompe di calore ad alta temperatura, mirandone ad ottimizzare le prestazioni e l'efficienza per l'utilizzo in applicazioni industriali. Una significativa innovazione consiste nella proposta di una soluzione tecnologica innovativa che preveda l'utilizzo di un espansore per migliorare il COP e recuperare parte del lavoro speso dal compressore. Le prestazioni di questi sistemi sono state analizzate su un ampio spettro di parametri operativi e presupposti impiantistici. I risultati, presentati attraverso mappe termiche per diverse configurazioni, dimostrano come l'utilizzo dell'espansore consenta COP significativamente più elevati con miglioramenti delle efficienze del secondo principio. Ciò porta a un vantaggio non solo per la produzione di energia ad alta temperatura, ma anche per i sistemi PTES, fornendo significativi benefici sulla RTE. Il lavoro coinvolge anche la calibrazione e la validazione di un modello numerico utilizzando l'Equazione di Stato di Peng-Robinson per definire le proprietà termodinamiche delle miscele. Vengono esaminati diversi casi di studio per proporre applicazioni efficienti, sia per HTHP che per PTES. L'intero studio, comprese le simulazioni numeriche e lo sviluppo del modello, è condotto utilizzando MATLAB.

Parole chiave: Pompe di Calore ad Alta Temperatura, Miscele a base di CO2, Peng-Robinson, Pumped Thermal Energy Storage (PTES)